KINETICS OF CORDIERITE FORMATION

A THESIS

Presented to

The Faculty of the Division of Graduate

Studies and Research

By

Geza Nicholas Zirczy

In Partial Fulfillment

of the Requirements for the Degree

Master of Science in Ceramic Engineering

Georgia Institute of Technology

August, 1972

In presenting the dissertation as a partial fulfillment of the requirements for an advanced degree from the Georgia Institute of Technology, I agree that the Library of the Institute shall make it available for inspection and circulation in accordance with its regulations governing materials of this type. I agree that permission to copy from, or to publish from, this dissertation may be granted by the professor under whose direction it was written, or, in his absence, by the Dean of the Graduate Division when such copying or publication is solely for scholarly purposes and does not involve potential financial gain. It is understood that any copying from, or publication of, this dissertation which involves potential financial gain will not be allowed without written permission.

7/25/68

KINETICS OF CORDIERITE FORMATION

Approved:

Dr. J. K. Cochran, Jr., Chairman

Dr. Lane Mitchell

Dr. A. T. Chapman

Date approved by Chairman: 8-10-72

ACKNOWLEDGEMENTS

I wish to express my appreciation to my wife, Helena, for the excellent typing of the draft and her constant encouragement throughout the course of this work.

In addition, I am deeply indebted to Dr. Joe K. Cochran, Jr. for his interest and help, especially his willingness to assist at any time throughout the course of this work.

Also, I thank Dr. Lane Mitchell and Dr. Allen T. Chapman for their cooperation as part of my reading committee.

I wish to thank Ceramica Carabobo, C.A., Valencia, Venezuela, for the funds which made this work possible.

I also wish to thank Mr. J. D. Parmelle, Harbison-Walker Refractories, Garber Research Center and Mr. D. F. Beal, Ferro Corporation, Technical Center, for their help. The raw materials for this work were generously furnished by Jim Archer, Glassrock Products Incorporated.

Finally, I wish to thank Mr. Thomas Machrovitch and Mr. Roberto Arrieta for their help in the preparation and firing of the samples.

TABLE OF CONTENTS

Page

ACKNOWLEDGEMENTS. ii

LIST OF TABLES v

LIST OF ILLUSTRATIONS. vi

SUMMARY. viii

Chapter

I. INTRODUCTION. 1

II. REVIEW OF THE LITERATURE. 3

Cordierite Crystal Structure
Reaction for Cordierite Formation
Properties of Cordierite Bodies
Solid State Reactions

III. PROCEDURE 22

Compositions
Mixing, Forming and Firing
Phase Analysis

IV. DISCUSSION OF RESULTS 29

Reaction of Spinel and Silica
Reactions of Forsterite, Mullite and Silica

V. CONCLUSIONS AND RECOMMENDATIONS 53

Conclusions
Recommendations

APPENDICES

A. RAW MATERIALS 55

B. PREPARATION OF CORDIERITE STANDARD 56

C. X-RAY QUALITATIVE ANALYSIS 57

TABLE OF CONTENTS (Continued)

Appendix Page

D. QUANTITATIVE X-RAY DIFFRACTION DATA 60

BIBLIOGRAPHY 65

LIST OF TABLES

Table		Page
1.	Invariant Points Surrounding the Cordierite Area	8
2.	Mean Thermal Expansion Coefficients for a Number of Materials	16
3.	Compositions of Cordierite Bodies	23
4.	Cordierite Content for Composition 1	30
5.	First Order Rate Constants for Cordierite Formation	31
6.	Activation Energy for Cordierite Formation	33
7.	Cordierite Content for Composition 2	41
8.	Cordierite Content for Compositions 1, 2, 3, 4, 5 and 6 after 24 hours	41
9.	Cordierite Content for Composition 5	42
10.	Phase Analysis for Compositions 3 and 6	49
11.	Raw Materials	55
12.	Composition Used in Preparing Cordierite Standard	56
13.	Experimental Conditions for Room Temperature X-rayDiffraction Analysis	58
14.	Experimental Conditions for High Temperature X-ray Diffraction Analysis	59
15.	Cordierite Content at 1250^{o}C	61
16.	Cordierite Content at 1300^{o}C	62
17.	Cordierite Content at 1350^{o}C	63
18.	Cordierite Content at 1400^{o}C	64

LIST OF ILLUSTRATIONS

Figure		Page
1.	Structure of Cordierite With its Six-Member Ring of Tetrahedra Viewed Down The c-axis.	4
2.	Region of the $MgO-Al_2O_3-SiO_2$ Phase Diagram Surrounding the Cordierite Area	7
3.	Reaction Mechanism of Cordierite Formation by Firing Talc and Kaolin	12
4.	Reaction Mechanism of Cordierite Formation by Firing $MgCO_3$, Al_2O_3 and Flint	12
5.	Interdiffusion of Two Crystalline Phases A and B.	20
6.	Cordierite Calibration Curve Based on Area Under the Peak.	26
7.	Cordierite Calibration Curve Based on Peak Height.	27
8.	First Order Reaction of Composition 1	32
9.	Reaction of Composition 1 From Which the Arrhenius Activation Energy May be Calculated	34
10.	First Order Reaction of Composition 2	37
11.	Reaction of Composition 2 From Which the Arrhenus Activation Energy May be Calculated	38
12.	Cordierite Content for Compositions 1 and 2 After 24 Hours	39
13.	Cordierite Content for Composition 4 and 5 After 24 Hours	40
14.	First Order Reaction of Composition 5	43
15.	Reaction of Composition 5 From Which the Arrhenius Activation Energy May be Calculated	44

LIST OF ILLUSTRATIONS (Continued)

Figure Page

16. Cordierite Content for Compositions 1 and 4 After 24 Hours. 46

17. Cordierite Content for Compositions 2 and 5 After 24 Hours. 47

18. Cordierite Content Produced by Reacting Compositions 3 and 6 for 24 Hours At Various Temperatures. 51

approximately the same particle size. Addition of 5% of zircon indicated an increase of the amount of cordierite developed between 1350^{o} and 1400^{o}C, but at 1350^{o}C and below, zircon was a detriment to cordierite formation for all reactions.

CHAPTER I

INTRODUCTION

Ceramic bodies approaching the theoretical composition of cordierite, $2MgO.2Al_2O_3.5SiO_2$, have a wide application in electroceramics and kiln furniture. Their main characteristics are high resistance to thermal shock and low coefficient of thermal expansion. The coefficient of thermal expansion depends on the quantity of the cordierite phase developed. Because of a narrow firing range, cordierite content is difficult to control. If the material is underfired, the cordierite structure does not develop sufficiently, and if it is overfired, mullite, forsterite and glass develop, which results in an increase of thermal expansion. The addition of zircon increases the firing range without materially affecting the thermal expansion or thermal shock resistance (1).

In the $MgO-Al_2O_3-SiO_2$ diagram, cordierite lies in the mullite primary phase. Cordierite is formed by solid state reaction with MgO, Al_2O_3 and SiO_2 or from materials containing these oxides, at temperatures between 1100^{o} and $1400^{o}C$. The mechanism of the formation of cordierite depends on the heating temperature, amount of impurities and the nature of the starting components. Previous work indicates that cordierite formation may depend on the presence of intermediate phases (2).

The purpose of this work was to investigate the reactions for cordierite formation. Using spinel, mullite, forsterite, fused silica, and zircon as the raw

material, reactions resulting in cordierite were studied in the temperature range 1200^{o} to 1400^{o}C. Through quantitative analysis, reaction rates and the temperature dependence of reaction rates were investigated to determine optimum firing conditions for various cordierite compositions.

CHAPTER II

REVIEW OF THE LITERATURE

Cordierite Crystal Structure

An investigation on the structure of cordierite was carried out by Gossner and Mussgnug (3). They found that the unit cell was orthorhombic with the edge lengths a = 17.10; b = 9.78; c = 9.33 Å. From the formula, $Mg_2Al_4Si_5O_{18}$, they assumed a pseudohexagonal structure of the Beryl type (beryl: $Be_3Al_2Si_6O_{18}$), with 2Mg + Al corresponding to 3Be and 5Si + Al to 6Si.

Figure 1 shows the crystal structure of cordierite viewed along the c-axis (3). This drawing emphasizes the six membered rings formed by silica tetrahedra which are joined by alumina tetrahedra and magnesia octahedron. Gibbs (4), has confirmed, for the most part, the ideal structure published by Byström (3) and has produced a more precise set of atomic parameters which clearly indicates an ordered alumina and silica arrangement. The tetrahedra bond angles of the silica and alumina tetrahedra average 109.5 and 110.2°, respectively, closely approximating the ideal tetrahedra angle of 109.47°. The angles within the tetrahedra comprising the six membered ring have a spread of values (105.6 - 114.6°) similar to those recorded for other silicates with ordered framework structures i.e., low albite = (102.67 - 116.07°) (4). The overall mean Si-O and Al-O bond distances, 1.614 and 1.748 Å, respectively, are in excellent agreement with the values 1.61 and 1.75 Å recorded for SiO_4 and AlO_4 tetrahedra in the framework silicates. The

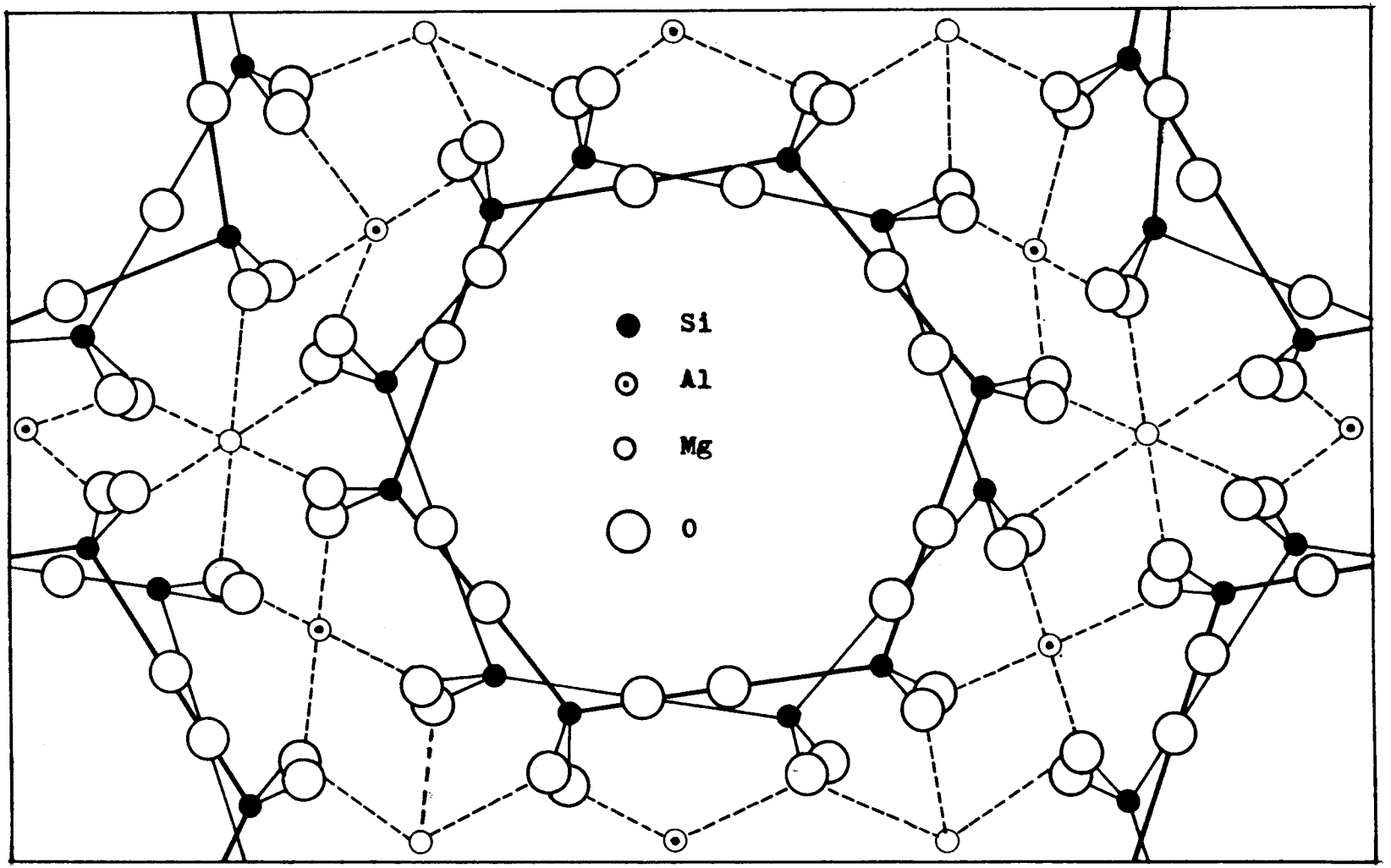

Figure 1. Structure of Cordierite with its Six-member Ring of Tetrahedra Viewed Down the c-axis.

individual Mg-O distances show a very small spread of values (between 2.113 and 2.124 $\mathring{A}$) and are not significantly different (4).

Karkhanavala and Hummel (5) considered that there exist three polymorphic modifications, α, β and μ, of cordierite. The stable high temperature (α) form can be easily obtained by solid state reaction of raw materials such as talc and kaolin at 1300°C to 1460°C or by crystallization of the glass at 1300°C for 24 hours. The stable low temperature modification (β) can be formed under hydrothermal conditions by crystallizing the glass at 655°C under a pressure of 10,000 lb. per sq. in. for 120 hours (5). The equilibrium inversion temperature of $\beta \rightarrow \alpha$ cordierite is given by Yoder as 830°C (6). A metastable low temperature modification (μ) can be obtained by devitrifying the glass around 850° at ordinary pressures for 360 hours (5). Miyashiro (7) found that high cordierite has a stable pseudohexagonal structure at high temperatures. High (α) cordierite has a lower refractive index than low (β) cordierite form, 1.524 and 1.537, respectively (5). The inversion of the (μ) form to the (α) cordierite occurs if held at 1010° for less than 5 minutes, or at 975° for about 2 hours. The inversion is irreversible at ordinary pressure, and the crystals of the high form do not revert to the low form in any reasonable time. This inversion of the (μ) form seemed to be variable with respect to the time temperature treatment (5). The (μ) form undergoes a considerable increase in volume while inverting to the high temperature form.

Reaction for Cordierite Formation

Cordierite bodies are used extensively in applications where low thermal expansion and good thermal shock resistance at moderate temperatures are desired.

Many questions, the mechanisms of cordierite formation, the structure of cordierite, the phase changes which occur in service, are incompletely answered. In actual practice, reactions forming cordierite in a ceramic body are complicated and empirical methods are used to determine the most suitable composition of a cordierite body. Two factors which interfere in the results are equilibrium which is rarely achieved when firing a ceramic body like cordierite and the proximity of six invariant points which surrounds the cordierite primary phase.

In firing cordierite, certain crystal formations, traceable back to the raw materials, remain unchanged in the fired article and have a pronounced effect upon the properties and crystal structure of the fired product. Furthermore, the raw materials used for cordierite bodies are by no means chemically pure, but contain impurities such as iron oxides, alkaline oxides, titanium dioxides, etc. These impurities may lower the firing temperature of the ceramic material and increase the amount of glassy matter in the fired product. Cordierite, the only stable ternary compound in the $MgO-Al_2O_3-SiO_2$ phase diagram (1), melts incongruently at $1460^{o}C$, accompanied by the formation of mullite and liquid (1). The theoretical composition of cordierite falls within the primary field of mullite, Fig. 2, but no mullite is present in such a body, unless it appears as a result of incomplete reaction or overfiring. Of course, mullite would be present in many other compositions within the mullite primary field. The region of the cordierite area is surrounded by six invariant points whose melting point and phases can be seen in Table 1. The invariant point with the highest temperature is produced by the composition mullite-sapphirine-cordierite and the lowest temperature

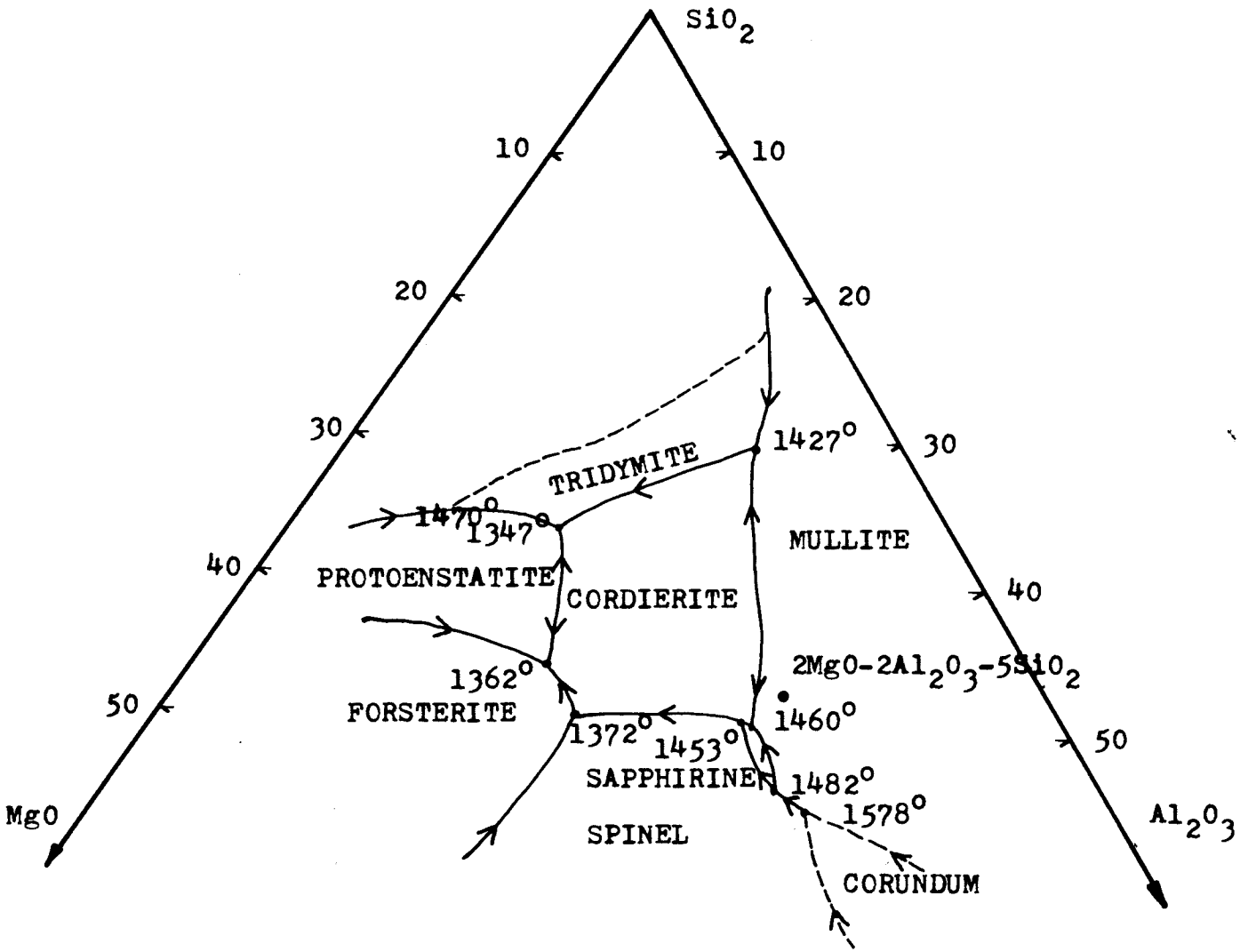

Figure 2. Region of The $MgO-Al_2O_3-SiO_2$ Phase Diagram Surrounding The Cordierite Area.

Table 1. Invariant Points Surrounding the Cordierite Area

Crystalline Phases	Composition (Wt. %) MgO	Al_2O_3	SiO_2	Temperature of Invariant Point (^{o}C)	Type of Invariant Point
Tridymite-Mullite -Cordierite	9.5	22.5	68.0	1427	Reaction
Mullite-Sapphirine -Cordierite	16.0	34.5	49.5	1460	Reaction
Sapphirine-Spinel -Cordierite	16.8	33.5	49.7	1453	Reaction
Spinel-Forsterite -Cordierite	25.7	22.5	51.8	1372	Reaction
Forsterite-Protoenstatite -Cordierite	25.0	21.0	54.0	1362	Eutectic
Protoenstatite-Tridymite -Cordierite	20.1	17.9	62.0	1347	Eutectic

formed by the composition protoenstatite-trydimite-cordierite. If a ceramic body with high refractoriness is desired, it has to be near the region of the invariant point formed by mullite-sapphirine-cordierite (8).

A serious disadvantage of many cordierite compositions is the narrow firing range. Underfiring fails to develop sufficient crystalline cordierite for low thermal expansion and high resistance to thermal shock. Overfiring results in the deterioration of crystalline cordierite into forsterite and mullite, which appreciably increases the thermal expansion (9). It is important to know the melting interval in the processing of ceramic bodies. With the exception of congruently melting compounds, all compositions have a melting interval, rather than a sharp melting point. It is this melting interval which largely determines the firing range of the body. The firing range is usually understood to be the temperature range between the attainment of vitrification and the development of bloating or distortion (10). The attainment of vitrification depends on the formation of a certain minimum percentage of liquid phase to provide a glassy bond. This minimum percentage of liquid may vary considerably, depending on such factors as the viscosity of the melt. Therefore, the relative amounts of crystalline and liquid phase, in addition to the temperature interval of melting, are important factors in determining the firing range. The firing range of a cordierite body can be extended by adding zircon without materially affecting the thermal expansion or thermal shock resistance. Zircon has a low coefficient of thermal expansion, and, reduces the temperature of cordierite formation.

The raw materials most frequently used in cordierite composition are clay,

talc and alumina. Talc liberates free-silica during firing which gives an increase of the thermal expansion coefficient and sometimes talc is substituted by magnesium carbonate and flint. Many commercial compositions do not approach the theoretical formula for cordierite but must fall within the following limits for cordierite formations (11):

$$45\% < SiO_2 < 63\%$$

$$23.5\% < Al_2O_3 < 44.5\%$$

$$6.5\% < MgO < 19.5\%$$

$$Al_2O_3 + MgO \geq 37\%$$

Krönert and others studied the reactions sequence leading to cordierite formation using two raw material compositions (2). Using a talc-kaolin reaction, Fig. 3, the products formed were represented by the following equations:

$$\underset{\text{(kaolin)}}{Al_2O_3 . 2SiO_2 . 2H_2O} \xrightarrow{800^\circ C} \underset{\text{(metakaolin)}}{Al_2O_3 . 2SiO_2} + H_2O \qquad (1)$$

$$\underset{\text{(talc)}}{3MgO . 4SiO_2 . H_2O} \xrightarrow{800^\circ C} \underset{\text{(protoenstatite)}}{3(MgO . SiO_2)} + \underset{\text{(amorphous silica)}}{SiO_2} + H_2O \qquad (2)$$

$$\underset{\text{(metakaolin)}}{(Al_2O_3 . 2SiO_2)} \xrightarrow{1000^\circ C} \underset{\text{(mullite)}}{3Al_2O_3 . 2SiO_2} + \underset{\text{(cristobalite)}}{4SiO_2} \qquad (3)$$

$$2(3Al_2O_3 \cdot 2SiO_2) + 5(SiO_2) + 6(MgO \cdot SiO_2) \xrightarrow{1150^{\circ}C} \quad (4)$$

(mullite) (Cristobalite) (Protoenstatite)

$$3(2MgO \cdot 2Al_2O_3 \cdot 5SiO_2)$$

(Cordierite)

From the talc-kaolin reaction intermediate phases of protoenstatite and mullite were present before cordierite formed. The second reaction sequence starting with magnesium carbonate, alumina and flint as raw materials, Fig. 4, was expressed by the following equations:

$$MgCO_3 \xrightarrow{800^{\circ}C} MgO + CO_2 \quad (5)$$

$$MgO + Al_2O_3 \xrightarrow{900^{\circ}C} (MgO \cdot Al_2O_3) \quad (6)$$

(Spinel)

$$SiO_2 \xrightarrow{1100^{\circ}C} SiO_2 \quad (7)$$

(Flint) (Cristobalite)

$$2(MgO \cdot Al_2O_3) + 5(SiO_2) \xrightarrow{1200^{\circ}C} 2MgO \cdot 2Al_2O_3 \cdot 5SiO_2 \quad (8)$$

(Spinel) (Cristobalite) (Cordierite)

From the magnesium carbonate, alumina and flint reaction, the intermediate spinel phase disappeared when cordierite started to crystallize at 1200°C. In both cases cristobalite started forming between 1000 - 1100°C and was consumed as cordierite crystallized.

Lamar and Warner (10) prepared ceramic bodies approaching the theoretical

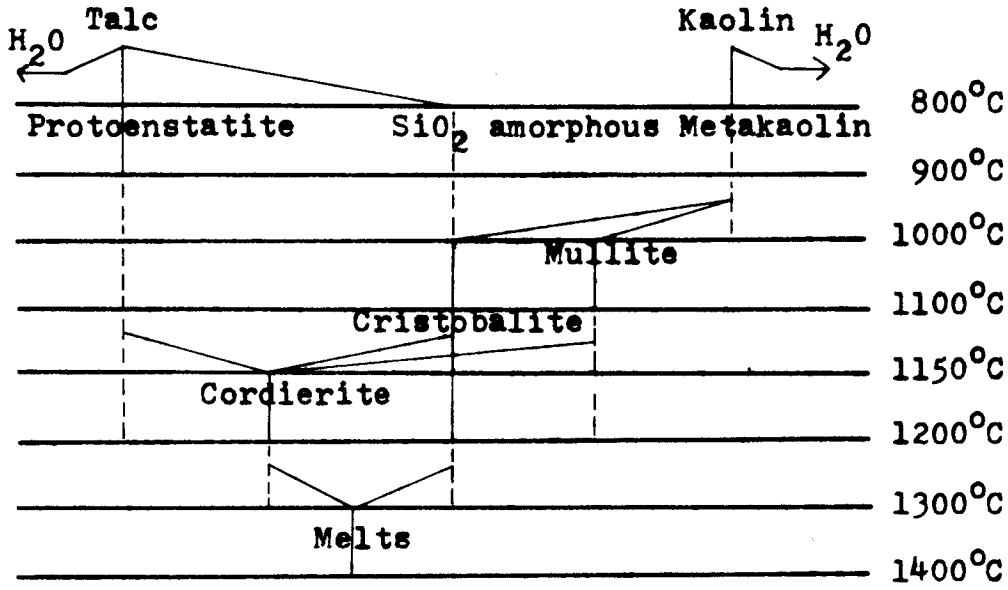

Figure 3. Reaction Mechanism of Cordierite Formation by Firing Talc and Kaolin.

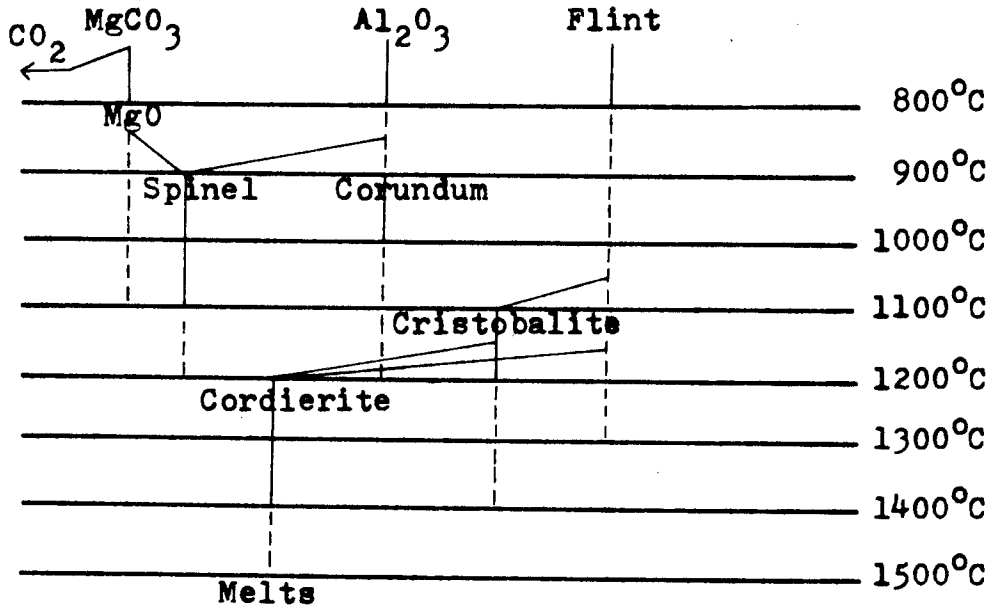

Figure 4. Reaction Mechanism of Cordierite Formation by Firing $MgCO_3$, Al_2O_3 and Flint.

composition of cordierite from mixtures of talc and clay. They concluded by means of DTA that cordierite forms by exothermic reaction at about 1300°C. Sorrel (12) considered that formation of mullite was responsible for this peak and the endothermic reaction at 1240°C and 1330°C corresponded to the formation of cordierite. Sorrel's bodies combined kaolin, ball clay, mullite, kyanite, silica-alumina grog, talc, and Sierralite. On DTA analysis, Sierralite and talc exhibited endothermic peaks with maxima at 1303° and 1330°C, respectively. Both endotherms were attributed to the formation of glass. Kaolin and ball clay reacted to form mullite as exhibited exothermic peaks at 1273° and 1205°C, respectively. The intensity of the mullitization of ball clay was less than that of kaolin and the dissociation occurred at a considerably lower temperature. The relatively poor crystallinity of the kaolinite in the ball clay and the greater proportion of impurities might be expected to lead to these results. The formation of cordierite was accompanied by a decrease in mullite content after the rate of reaction became greater than the rate of mullitization, as between 1150° and 1200°C. Cordierite formation was attributed to an endotherm at 1238°C.

According to Sorrel (12), formation of cordierite depended on the quantity of mullite, because the crystallization rate depended on it. From DTA and x-ray diffraction studies of the reaction sequence in cordierite formation, Sorrel (12) concluded that the availability of mullite is the main factor in forming cordierite. This implied that dehydrated kaolinite does not react directly with the magnestitic material to form cordierite; consequently the firing temperature, chemical composition and crystal structure are largely responsible for cordierite formation.

However, the conclusion that mullite is necessary for cordierite formation must be limited to bodies that are formed with clay, since Krönert and others showed that mullite does not form when starting with magnesium carbonate, alumina and flint.

Properties of Cordierite Bodies

Thermal Expansion

Thermal expansion is related to atomic vibrations. If each atom oscillates with increasing amplitude as the temperature rises, it must repel its neighbors in order to acquire the necessary space for its movement, and the result will appear externally as an expansion of the body. Thermal expansion is simply an external record of the increase in amplitude of the longest vibrations, whereas the increase in energy must be distributed throughout all the modes of vibration. Each atom or molecule in a crystal is permanently located at the lattice point and vibrates constantly about its average position (13).

The mineral cordierite has an anisotropic thermal expansion which is positive in the c-direction, and negative in the a and b directions. Cordierite specimens containing crystals in random orientation will exhibit coefficients of linear thermal expansion from 1.5 to 3.5 x 10^{-6}, depending upon the degree of purity and the nature of the impurities (14). Low thermal expansion is of special interest because thermal shock resistance of a ceramic material depends on the thermal expansion coefficient. Beals and Cook (14) observed a close correlation between the cordierite content and the thermal expansion behavior of the bodies. For any body, the increase in cordierite content resulted in a decrease in the coefficient

of expansion. The lowest coefficient of linear thermal expansion observed was 9.8×10^{-7} for the range 20^{o} to 300^{o}C. The composition in weight percent of this body was 47.91 talc, 39.27 kaolin, and 12.82 alumina. Crystalline cordierite was present as 96% of the composition upon firing to 1400^{o}C. When this composition was fired to 1350^{o}C, analysis showed 90% cordierite and a coefficient of expansion of 10.8×10^{-7}. Davis and Hackler (15) found that the linear thermal expansion of mullite and cordierite bodies is dominated by the expansion of cordierite.

The need for materials possessing low thermal expansion and capable of withstanding high temperatures has become important in the field of electronics. Comparison of cordierite to other commonly used ceramic materials, Table 2, shows that only fused silica has a lower thermal expansion. Fused silica undergoes a phase transformation at 1100^{o}C to cristobalite which has a high thermal expansion coefficient. This fused silica to cristobalite transformation has severely limited the use of fused silica as a low expansion refractory material.

Thermal Shock Resistance

Thermal shock is produced when a body is heated or cooled so rapidly that very high transient temperature gradients are set up. A ceramic body with low thermal conductivity which is subjected to rapid temperature change readily produces high temperature gradients. This in turn leads to differential expansion within the body because the rapidly heated or cooled face expands or contracts less than the respectively cooler or hotter parts of the body. The strain induced increases with thermal expansion coefficient, which is an important factor in determining resistance to thermal shock (17). Schott and Winckelmann (18) established

Table 2. Mean Thermal Expansion Coefficients for a Number of Materials (16)

Material	Linear Expansion Coefficient 0-1000°C x 10^{-6}
Fused Silica glass	0.5
Cordierite	1.0
Zircon	4.2
SiC	4.7
Mullite	5.3
Spinel	7.6
Steatite	8.7
Al_2O_3	8.8
Forsterite	10.8
MgO	13.5
Quartz	14.0
Cristobalite	17.0

an empirical formula to grade the thermal shock resistance for ceramic materials.

$$W = \frac{T}{E \cdot n} \sqrt{\frac{K}{p \cdot c}} \qquad (9)$$

where:

W = thermal shock resistance

T = tensile strength

E = modulus of elasticity

n = coefficient of thermal expansion

K = thermal conductivity

p = specific gravity

c = specific heat

The formula states that a material of good thermal shock resistance has to be of low modulus of elasticity, low coefficient of thermal expansion, high thermal conductivity, low heat capacity. Unfortunately, only thermal expansion and thermal conductivity can be varied to an appreciable extent. The ability to withstand sudden temperature changes without cracking is an important requirement for many ceramic applications but is a property hard to obtain. One method of improving the shock resistance is to lower the coefficient of thermal expansion by the formation of cordierite. Care must be taken to assure firing at a high enough temperature to bring this final reaction to completion. Otherwise the cristobalite remaining will prevent the body from having the desired low thermal expansion. Porous materials usually withstand thermal shock better than dense ones, but porous materials are seldom used for chemical applications and the electrical industries are mostly interested in dense materials of high mechanical strength and good electrical properties like cordierite.

Solid State Reactions

Cordierite formation is a solid state reaction. Reactions between solids in the absence of a liquid phase to form a new phase involve diffusion process, which depends on time, particle size and temperature. Solid state reactions are carried out by intimately mixing fine powders. The reaction rate increases exponentially with temperature. Before any chemical reaction can occur, the reacting atoms must acquire a certain minimum thermal energy or an activation energy.

The rate of a reaction is usually expressed as the rate of change of the

concentration of the reactants with time, at a constant temperature (19). The rate law for the reaction can be determined only by experimental kinetic studies and cannot be deduced from the balanced chemical equation. The first-order kinetic law, has the following equation (19):

$$\frac{dA}{dt} = -K\,(A) \qquad (10)$$

Equation (10) corresponds to the statement that the rate of reaction at any time is proportional to the amount unchanged at that time. The first-order rate constant could be calculated from the following equation:

$$\log\,(A) = -\frac{Kt}{2.303} + \log\,(Ao) \qquad (11)$$

where:

A = amount of the reactant at time (t)

K = reaction rate constant (sec^{-1})

t = time

The rate constant K may be calculated from a plot of log (A) versus t; the slope of such a plot is -K/2.303.

The temperature dependence of rate processes is usually expressed by the Arrhenius relationship which states that the logarithm of the reaction rate constant K is proportional to the reciprocal of the absolute temperature.

$$K = A\ e^{\frac{-Ea}{RT}} \qquad (12)$$

where:

K = rate constant

Ea = activation energy $\frac{(\text{calories})}{\text{mole}}$

T = absolute temperature (^{o}K)

R = gas constant $\frac{(1.99 \text{ calories})}{^{o}C \times \text{mole}}$

The exponential term in equation (12) expresses the fraction of remaining reactants reacting at any instant (17). The Arrhenius relationship makes no assumption of the type of reaction involved. The temperature dependence of the velocity of a solid phase reaction is primarily determined by the energy of activation, or "work of loosening" of the constituents.

An important factor in controlling reaction speed is particle size. Since reaction between solids in contact involve ionic or atomic interchange between crystal phases, it is obvious that diffusion phenomena within crystals will play an important role. The present concept would, therefore, be that where the bonds between two kinds of atoms or ions are weak, diffusion will be high. As the bond strength increases, the diffusion coefficient falls off and the influence of temperature becomes greater (20). Two solid phases, A and B are considered to be in contact, as represented in Figure 5 shown on the next page.

The figure represents the successive stages in the diffusion process and the progressive widening of the diffusion band. Initially atom B on the phase boundary finds it easier to diffuse into the adjacent phase than into its own because

Initial stage	A	A	A	A	A	A	A	B	B	B	B	B	B	B
First step	A	A	A	A	A	A	B	A	B	B	B	B	B	B
Second step	A	A	A	A	A	B	A	B	A	B	B	B	B	B
Third step	A	A	A	A	B	A	B	A	B	A	B	B	B	B
Fourth step	A	A	A	B	A	B	A	B	A	B	A	B	B	B

Figure 5. Interdiffusion of Two Crystalline Phases A and B.

its thermodynamic activity in the adjacent phase is zero and the process of diffusion will involve a large free-energy decrease. The same reasoning applies to atom A on the phase boundary. Accordingly the first step is taken and we now have two phase boundaries instead of one. On the left atom A interchanges with its neighbor B across the boundary, and on the right atom B interchanges with its neighbor A across the other boundary. We now have the second stage. The process repeats until A and B have completely reacted to form AB or at least until one of the components is exhausted. It will be seen that in every case the phase boundaries are the active zones where the reaction process is initiated. It is to be noted, however, that with every advance of the boundaries into phases A and B, interchanges of atomic positions occur within the reaction product AB. This postulates that in the solid product, AB, the constituents atoms are loosely bound at the temperature that rapid diffusion is occurring. If they are tightly bound the freedom of this interchange will be diminished. If a high melting product is formed the reaction

will tend to be slow unless the temperature is raised accordingly. On the other hand, if the reaction product, AB, shows a transition temperature (where internal rearrangement is occurring), the mutual diffusion of A and B may prove to be very rapid (20).

CHAPTER III

PROCEDURE

Compositions

In this study six ceramic bodies were prepared from mixtures of spinel, fused silica, forsterite, mullite and zircon. These compositions were calculated approaching the theoretical composition of cordierite. The composition of the bodies are given in Table 3. The particle size of the raw materials which enters in each composition are given in Appendix A.

Mixing, Forming and Firing

Bodies were prepared by mixing the ingredients in distilled water for 20 minutes in a high speed blender and then filtered on paper. The residues were dried at 120^{o}C for 12 hours. The dried slurries were passed through a 40 mesh sieve. Bars, one-fourth by one-fourth by four inches were pressed in a steel die to 15, 000 pounds per square inch using polyvinil alcohol as a binder. The press was a hydraulic type Carver laboratory model.

The samples were fired in a laboratory kiln equipped with Globar elements. Compositions 1, 2, 3, 4, 5 and 6 were quench heated to 1250^{o}, 1300^{o}, 1350^{o}, 1400^{o}C and quenched in air after 24 hours. Compositions 1, 2 and 5 were quenched in air after 2, 4, 10 and 24 hours. The samples were labeled 1-2, 1-4, 1-10 and 1-24. The first number represented the composition and the second denoted hours

Table 3. Compositions of Cordierite Bodies

Composition	Raw Material	Weight Percent
1	Spinel	48.6
	Fused Silica	51.4
2	Spinel	48.6
	Fused Silica	51.4
	Fused Silica (excess)	5.0
3	Forsterite	24.1
	Mullite	48.5
	Fused Silica	27.4
4	Composition 1	100.0
	Zircon	5.0
5	Composition 2	100.0
	Zircon	5.0
6	Composition 3	100.0
	Zircon	5.0

of firing.

Phase Analysis

Phase analysis were made using a Norelco x-ray diffractometer equipped with a copper target using maximum slit openings with damping and amplitude adjusted to give a fairly smooth background and to keep the most intense peak on scale. All samples of x-ray analysis were ground to 325 mesh with a Fisher automatic mortar grinder and mounted for x-ray diffraction analysis using an appropriate method to limit preferred orientation and insure a smooth uniform surface.

Preparation of Standard Curves

Strontium fluoride was used as the internal standard in this study. A fairly well-defined peak with no super-imposed peaks at the Bragg angle of 10.42^{o} was chosen for cordierite, and the peak at 52.22^{o} was used for strontium fluoride. Data for establishing a calibration curve of the amount of cordierite present in a sample as indicated by the ratio of the height and area of the cordierite peak to that of the strontium fluoride peak were obtained in the following manner:
A standard sample of 100% crystalline cordierite, Appendix B, was mixed with fused silica in varying proportions to form a calibration sample. To each 100 parts of the mixture of cordierite and fused silica, 20 parts of strontium fluoride were added. Peak height was measured from the background. To determine peak area, total counts were recorded in scanning from 9.75 to 11.00 2θ degrees for cordierite, and 51.75 to 53.00 2θ degrees for SrF_2. Background counts for the respective peaks were recorded by counting for five minutes at 9.75 and 51.75 2θ

degrees. The difference between counts recorded for scanning the peaks and the background counts was used as the peak areas. Ratios of the peak height and area of cordierite to those of the internal standard were calculated and plotted against the percentage of cordierite known to be present in the standard samples. The plot of these ratios established the calibration curve for cordierite, Figs. 6 and 7.

Quantitative Phase Analysis

Quantitative x-ray work was done using the experimental conditions outlined in Appendix C. The two most important factors for true and reproducible results in quantitative x-ray diffraction are small particle size and homogeneity of the sample. Intensity variations between runs of the same sample may have been due to preferred orientation and lack of homogeneity. The samples for analysis were prepared by intimately mixing 1 gram of the sample with 0.2 gram of the internal standard on an automatic shaker. The materials were analyzed in the same manner as were the standard samples and percent crystalline cordierite present in the fired bodies was determined from the calibration curves. Quantitative phase analysis was done for all the compositions.

Qualitative Phase Analysis

An important feature of this study is a knowledge of the crystalline phases present at each test temperature. In order to determine this, room temperature x-ray diffraction patterns were run from 10 to 70 2θ degrees on all compositions fired for 24 hours. Experimental conditions for room temperature qualitative x-ray diffraction analysis are given in Appendix C.

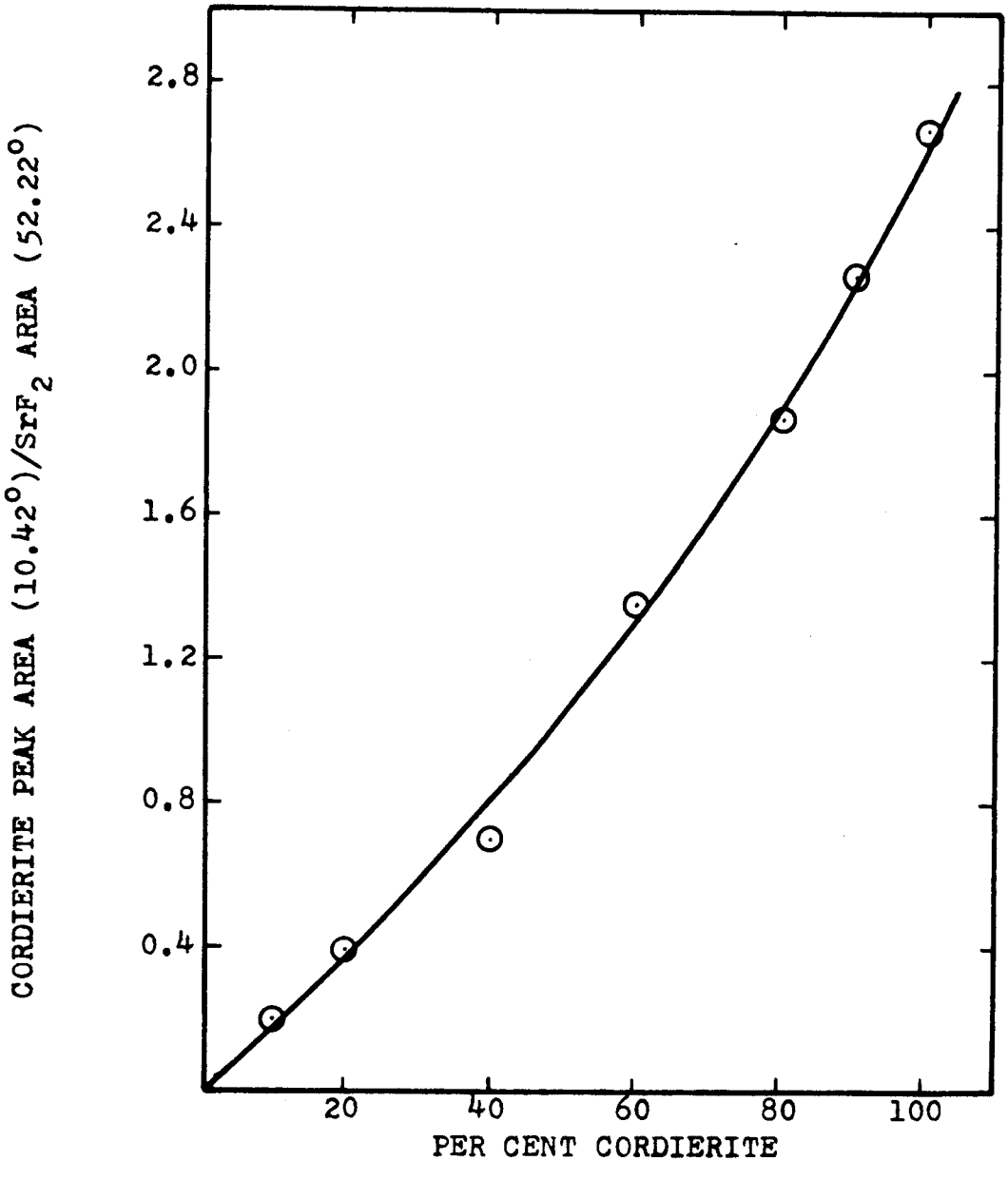

Figure 6. Cordierite Calibration Curve Based on Area Under The Peak.

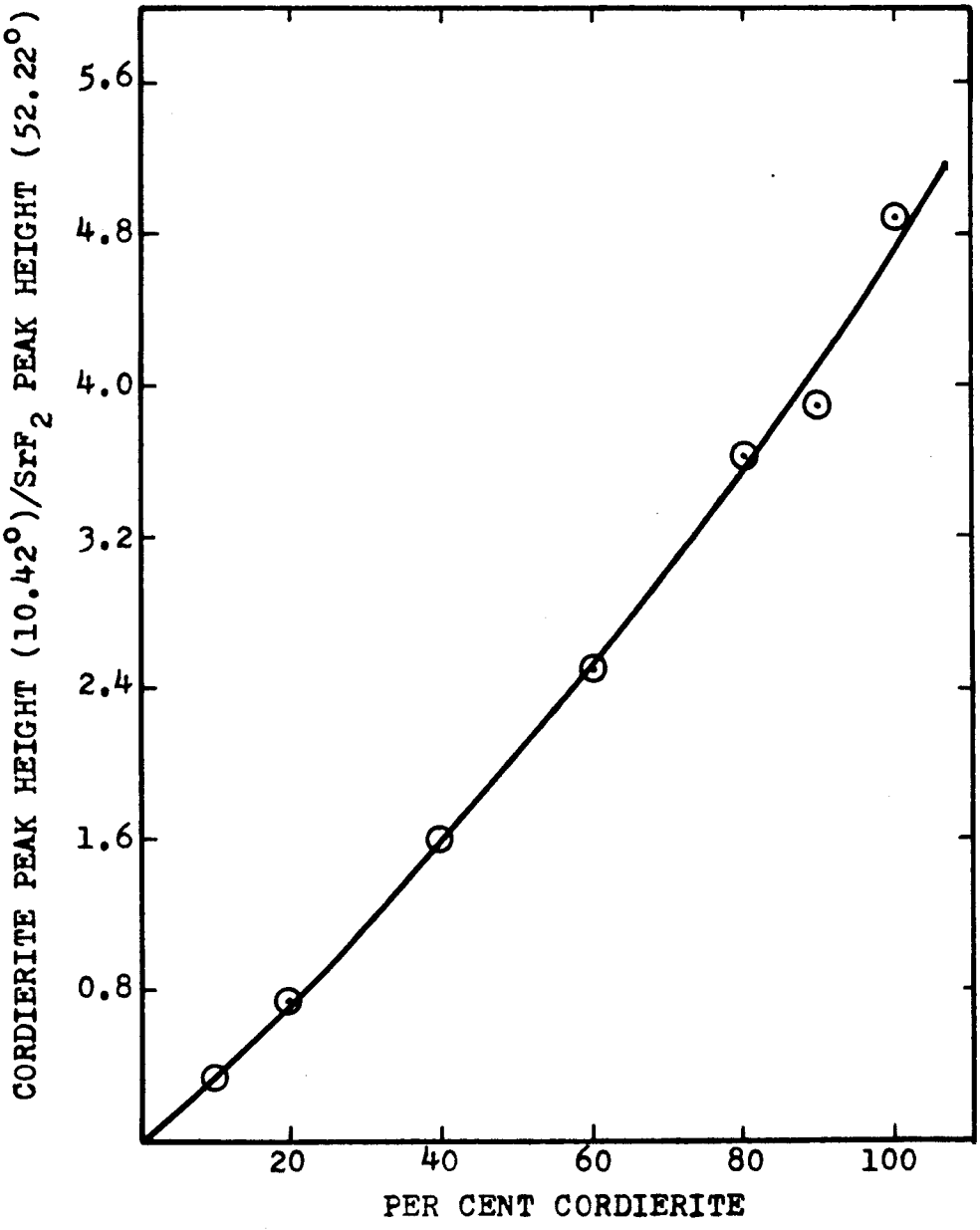

Figure 7. Cordierite Calibration Curve Based on Peak Height

High temperature x-ray analysis was done by Harbison Walker Refractories, Garber Research Center (21), for compositions 1, 2 and 5 in order to see the temperatures at which cordierite formation increases and to identify the phases present as cordierite develops. Runs were taken at 1200^{o}, 1250^{o}, 1275^{o}, 1300^{o}, 1325^{o} and 1350^{o}C. X-ray diffraction patterns were run from 5 to 70 2θ degrees. Runs were taken at room temperature before heating to 1200^{o}C and after heating to 1350^{o}C. Experimental conditions for high temperature x-ray diffraction analysis are given in Appendix C.

CHAPTER IV

DISCUSSION OF RESULTS

The primary objective of this research was to study the reaction sequence by which cordierite is formed based on phase analysis and reaction rates. Intermediate phases responsible for cordierite formation are discussed. Two basic reactant formulations were investigated: (1) spinel and fused silica, and (2) mullite, forsterite and fused silica. The effect of the addition of zircon and excess silica are considered. Combined results from these studies and previous work are used to modify or substantiate previously proposed theories and suggest optimum conditions for cordierite formation.

Reaction of Spinel and Silica

High Temperature X-ray Analysis

High temperature x-ray analysis of the phases present on reacting spinel with fused silica in stoichiometric ratios (composition 1), in the presence of five percent excess silica (composition 2), and with five percent zircon (composition 5) indicated the same results on a qualitative basis. The high temperature x-ray diffraction pattern showed cordierite formation at 1200^{o}C. Cristobalite was present at this temperature, so cordierite formation may have been due to reaction of spinel with fused silica and/or cristobalite. Other than the initial reactants, cordierite, and cristobalite, no other phases were detectable. Cristobalite formed

in this composition, as in all the other compositions, was the result of the devitrification of the fused silica used as a raw material.

During the balance of the temperatures heating schedule (1200°, 1250°, 1275°, 1300°, 1325° and 1350°C), cordierite increased in concentration at the expense of cristobalite and spinel. No mullite was detected at any temperature. Transmitted light examination of the sample, after heating, showed them to be composed of spinel and cordierite. Spinel crystal sizes ranged from approximately 10 to 40 microns; cordierite crystals were less than 5 microns diameter.

Reaction Mechanisms and Kinetics

Stoichiometric Reactants (Composition 1). Room temperature x-ray diffraction patterns gave the same results as given by high temperature x-ray. The only crystalline phases present at any temperature were spinel, cristobalite and cordierite. As the temperature increased from 1250°C to 1400°C, the cordierite phase increased and the spinel and cristobalite phase decreased. Cordierite content increased continuously with time and temperature as shown in Table 4.

Table 4. Cordierite Content for Composition 1
(Weight Percent)

Temperature (°C)	Time (Hours)			
	2	4	10	24
1250	11.5	12.0	15.0	18.5
1300	15.0	15.0	21.0	28.0
1350	20.0	23.0	27.0	37.5
1400	27.5	33.0	41.0	51.5

In an attempt to determine the reaction mechanisms for cordierite formation, with respect to spinel, Figure 8, the reaction rates between spinel and cristobalite leading to cordierite formation were determined experimentally. Spinel at any time was calculated from m-2n where m was original number of moles of spinel and n was moles of cordierite formed. By considering the quantity of the original reactants to be 584 gr., the molecular weight of cordierite, the weight fraction of cordierite at any time was equivalent to the number of moles of cordierite. Under these conditions, the original spinel content was two moles according to:

$$2(MgO.Al_2O_3) + 5SiO_2 \rightarrow 2MgO.2Al_2O_3.5SiO_2 \qquad (13)$$

By graphing the log (spinel) vs. time, the reaction with respect to spinel was forced to fit a first order reaction, and the rate constant, K, was calculated from the slope, Table 5.

Table 5. First Order Rate Constants for Cordierite Formation

Temperatures (^{o}C)	Composition		
	1	2	3
1250	4.00×10^{-3}	3.77×10^{-3}	3.97×10^{-3}
1300	7.52×10^{-3}	7.53×10^{-3}	6.48×10^{-3}
1350	1.08×10^{-2}	1.97×10^{-2}	1.20×10^{-2}
1400	1.88×10^{-2}	3.10×10^{-2}	2.39×10^{-2}

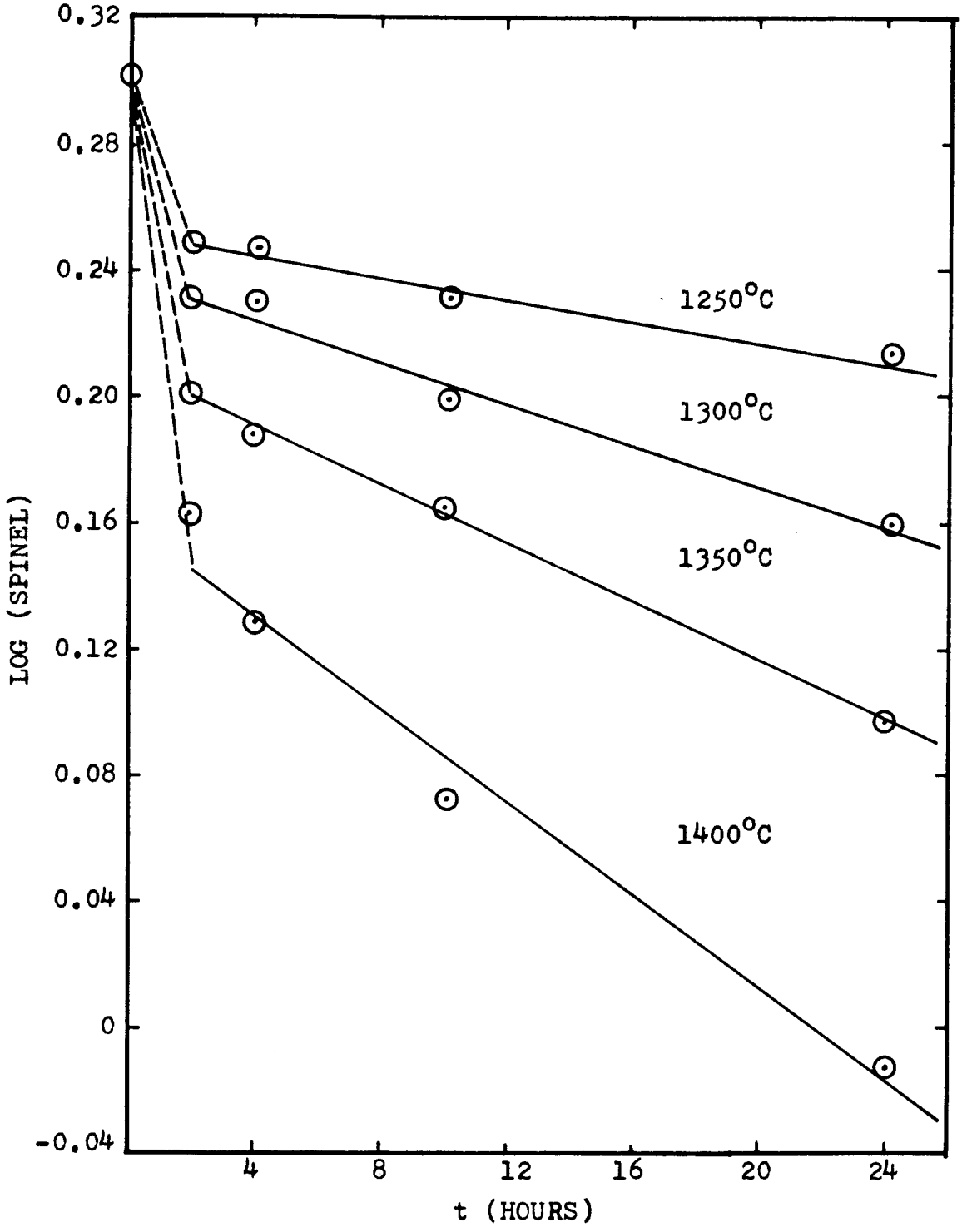

Figure 8. First Order Reaction of Composition (1).

Activation energy for cordierite formation was calculated from a standard Arrhenius curve, Figure 9. Activation energy for cordierite formation of composition 1 was 48.8 Kcalories/mole, Table 6.

Table 6. Activation Energy for Cordierite Formation

Compositions	Activation Energy (Kcalories/Mole)
1	48.8
2	74.7
5	57.5

From the results of x-ray analysis, the phases present allowed only the following reactions for cordierite formation using spinel and fused silica as the reactants:

$$2(MgO.Al_2O_3) + 5SiO_{2(g)} \longrightarrow 2MgO.2Al_2O_3.5SiO_2 \quad (14)$$

$$SiO_{2(g)} \longrightarrow SiO_{2(c)} \quad (15)$$

$$2(MgO.Al_2O_3) + 5SiO_{2(c)} \longrightarrow 2MgO.2Al_2O_3.5SiO_2 \quad (16)$$

where the subscripts (g) and (c) refer to glass and cristobalite. The slope change shown in Figure 8, during the first two hours, indicated that the reaction mechanism changed presumably from reaction (14) to (16) as reaction (15) proceeded. Evidence for this were the following:

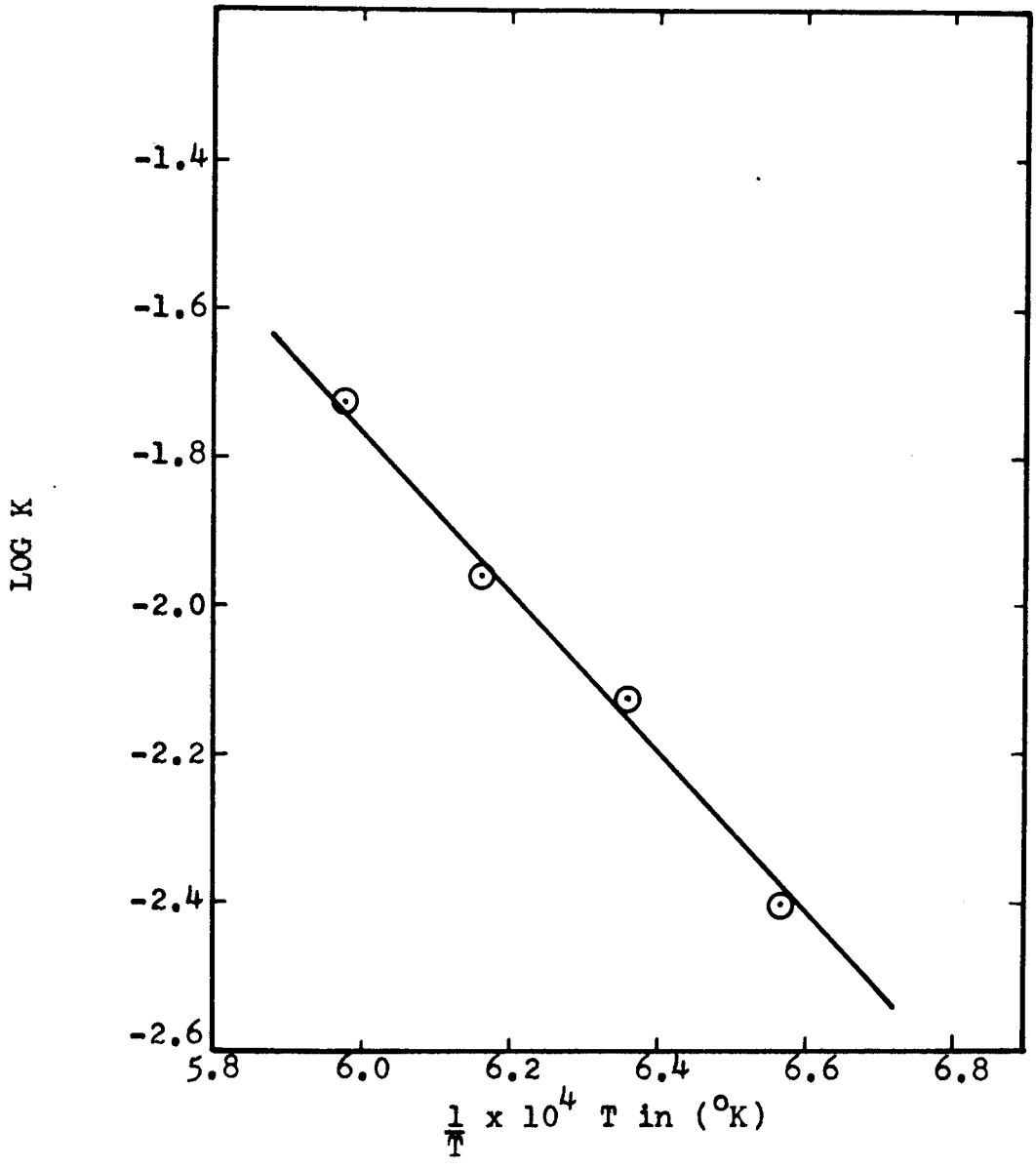

Figure 9. Reaction of Composition (1) From Which The Arrhenius Activation Energy May Be Calculated.

1. The initial reaction was assumed to be (14) because silica glass was used as a raw material.

2. Large quantities of cristobalite were detected by x-ray diffraction in the two hour firings, as a result of devitrification of silica glass which confirms reaction (15).

3. The only phases detected at any temperature for these compositions, by means of x-ray diffraction were spinel, cristobalite and cordierite.

A greater slope during the first two hours compared to longer times, Fig. 8, indicated that reaction in equation (14) is much faster than reaction (16). This is because silica glass is a metastable state which has much higher Gibbs free energy than the more stable cristobalite. The rate of devitrification of the glassy phase is a function of the temperature and the other constituents. In order to form cristobalite from silica glass, considerable motion of the silica tetrahedra is necessary. High viscosity of a glassy phase indicates a high degree of association and lack of free mobility of the tetrahedra, therefore, reducing the rate, and hence the amount of cristobalite formed. Impurities tend to increase the amount and rate of devitrification of the glassy phase by decreasing the viscosity and increasing the mobility of the silica tetrahedra or, by producing centers of ionic assymmetry which are effective in causing nucleation (21). In this case, spinel would serve to increase the rate of devitrification of the fused silica.

Effect of Silica Addition. Silica was added in excess to composition 2 in an effort to drive the spinel to form cordierite at a faster rate. With an addition of five percent excess silica and considering the total batch to weigh 584 grams, as was done for composition 1, the reaction for forming cordierite may be formulated as:

$$1.906(MgO.Al_2O_3) + 5.223SiO_2 \longrightarrow$$
$$0.953(2MgO.2Al_2O_3.5SiO_2) + 0.458SiO_2 \quad (17)$$

The amount of spinel at any time in composition 2 was calculated from m-2n where m was 1.906 moles of spinel and n was moles of cordierite formed, Table 7. Reaction rates were determined as previously described, Fig. 10, and activation energy for cordierite formation of composition 2 was 74.7 Kcalories/mole, Fig. 11.

From the results of the previous sections, composition 2 which contains excess silica, behaved approximately the same during heating as composition 1. Initial reaction was spinel and fused silica and later changed to spinel and cristobalite as indicated by the slope changes in Fig. 10.

To compare the effect of excess silica, composition 5 may be compared to composition 4 in addition to comparing composition 2 to composition 1, since the only difference in the two sets of reactions was the silica content. The amount of crystalline cordierite developed was less for compositions 2 and 5 than for compositions 1 and 4, Figs. 12 and 13, and this is due to the presence of excess silica that reduced the cordierite content for compositions 2 and 5. Comparing compositions 1 and 2 showed that there were higher reaction rates with excess silica above 1250^{o}C, Table 5, but because the quantity of spinel available to form cordierite has been diluted, the percentage cordierite formed is less with added silica. (See Table 8 for comparison of 24 hour cordierite contents). It had been hoped that adding excess silica would produce a sufficient increase in reaction rate to more than compensate for reduced spinel concentration. This did not happen.

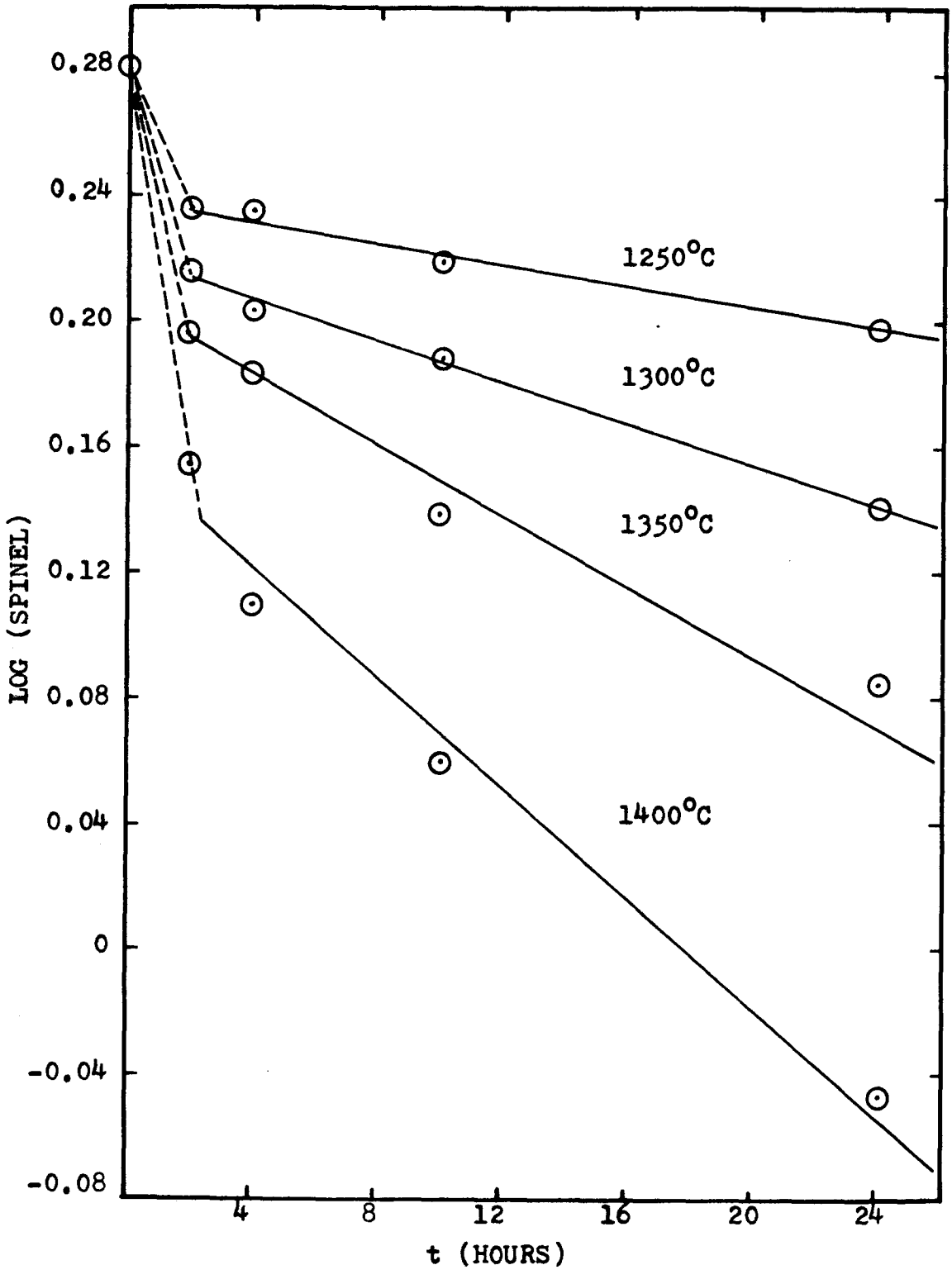

Figure 10. First Order Reaction of Composition (2)

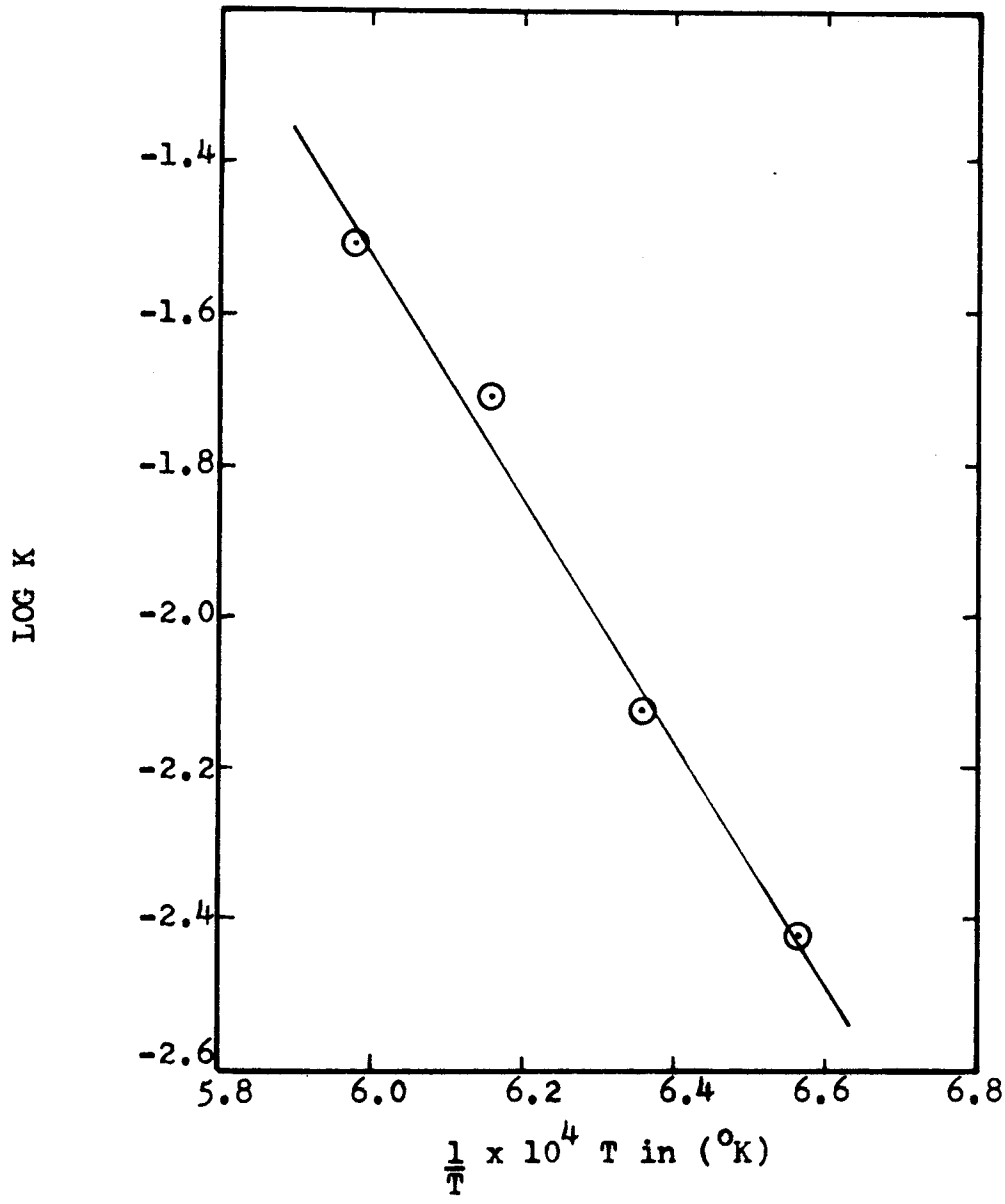

Figure 11. Reaction of Composition (2) From Which The Arrhenius Activation Energy May Be Calculated.

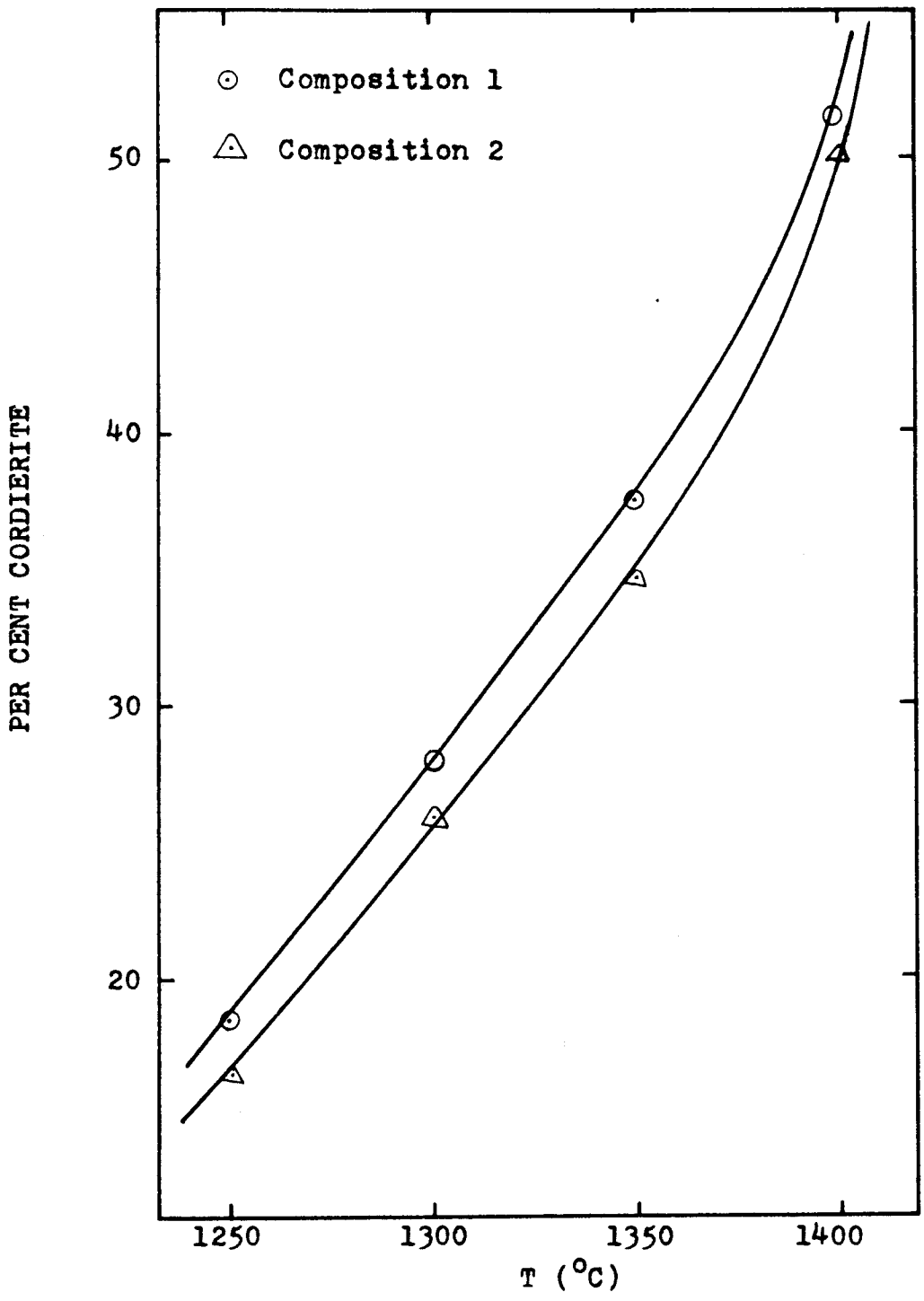

Figure 12. Cordierite Content for Compositions (1) and (2) After 24 Hours.

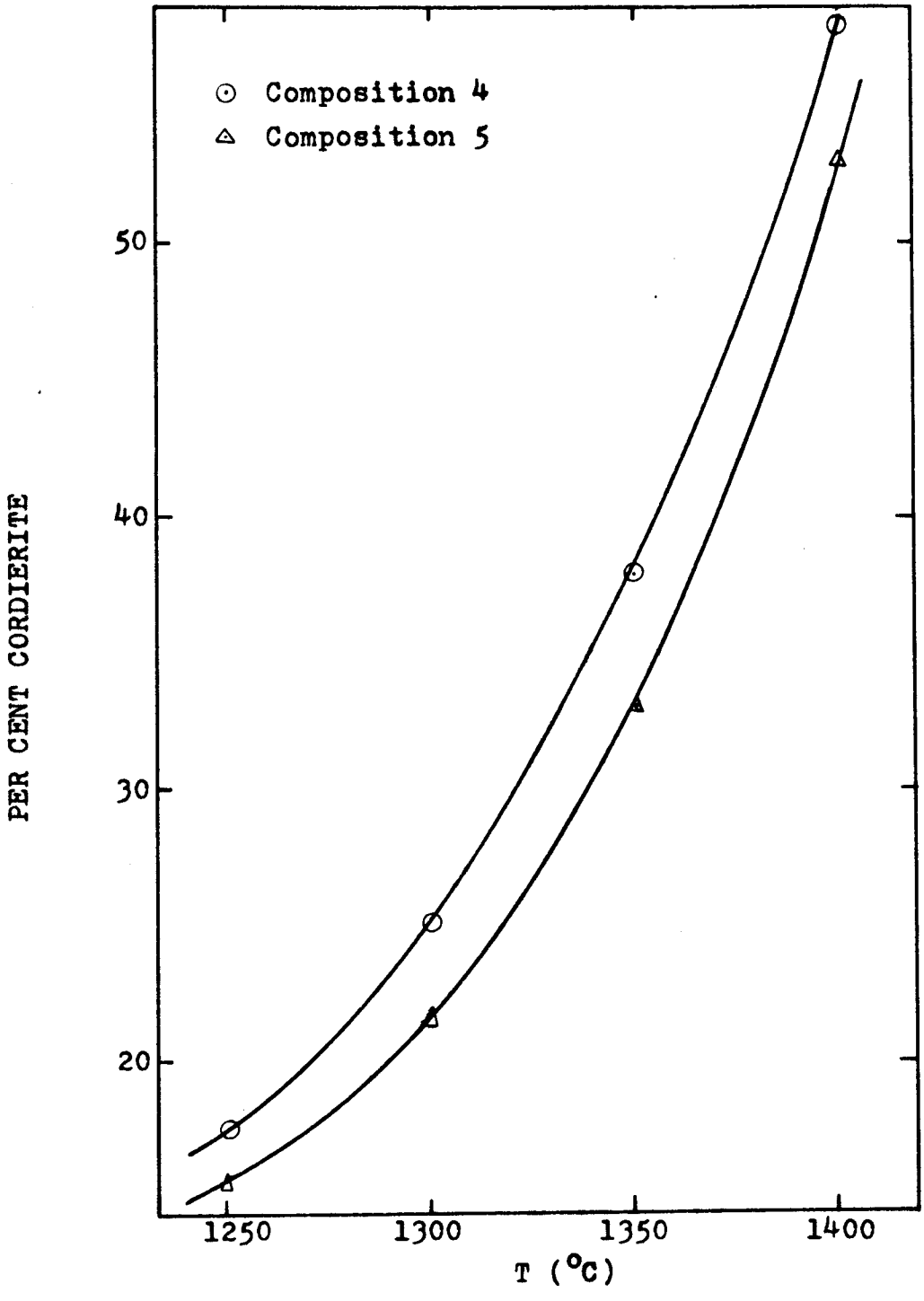

Figure 13. Cordierite Content for Compositions (4) and (5) After 24 Hours.

Table 7. Cordierite Content for Composition 2
(Weight percent)

Temperature (°C)	Time (Hours)			
	2	4	10	24
1250	9.5	11.5	12.5	16.5
1300	13.0	15.5	18.0	26.0
1350	17.0	19.0	26.5	34.5
1400	24.0	31.0	38.0	50.5

Table 8. Cordierite Content for Compositions
1, 2, 3, 4, 5 and 6 after 24 Hours.

Temperature (°C)	Compositions					
	1	2	3	4	5	6
1250	18.5	16.5	24.0	17.5	15.5	22.0
1300	28.0	26.0	37.5	25.0	21.5	37.5
1350	37.5	34.5	64.5	38.0	33.0	62.0
1400	51.5	50.5	76.5	58.0	53.0	78.5

Effect of Zircon Addition. Zircon was added to composition 5 to promote cordierite formation because of the previous work by Lamar (1). With an addition of five percent zircon and considering the total batch to weigh 584 grams, as was done for composition 1, the reaction for forming cordierite may be formulated as:

$$1.818(MgO.Al_2O_3) + 4.996SiO_2 + .145ZrSiO_4 \longrightarrow \quad (18)$$
$$.909(2MgO.2Al_2O_3.5SiO_2) + .451SiO_2 + .145ZrSiO_4$$

The amount of spinel at any time in composition 5 was calculated from m-2n where m was 1.818 moles of spinel and n was moles of cordierite formed as shown in Table 9.

Table 9. Cordierite Content for Composition 5
(Weight Percent)

Temperature (^{o}C)	Time (Hours)			
	2	4	10	24
1250	9.5	10.5	13.5	15.5
1300	12.5	13.0	18.0	21.5
1350	18.0	21.0	26.5	33.0
1400	28.0	30.0	40.5	53.0

Spinel concentration as a function of time was graphed as a first order reaction, Fig. 14. Activation energy for cordierite formation of composition 5 was 57.5 Kcalories/mole, Fig. 15. The results obtained in Table 6 showed that addition of excess silica increased the activation energy for cordierite reaction and zircon decreased it. Higher activation energies indicated that the reaction rate was increasing at a faster rate with temperature.

From the results of the previous sections, composition 5, which contains zircon, behaved approximately the same during heating as composition 1 and 2.

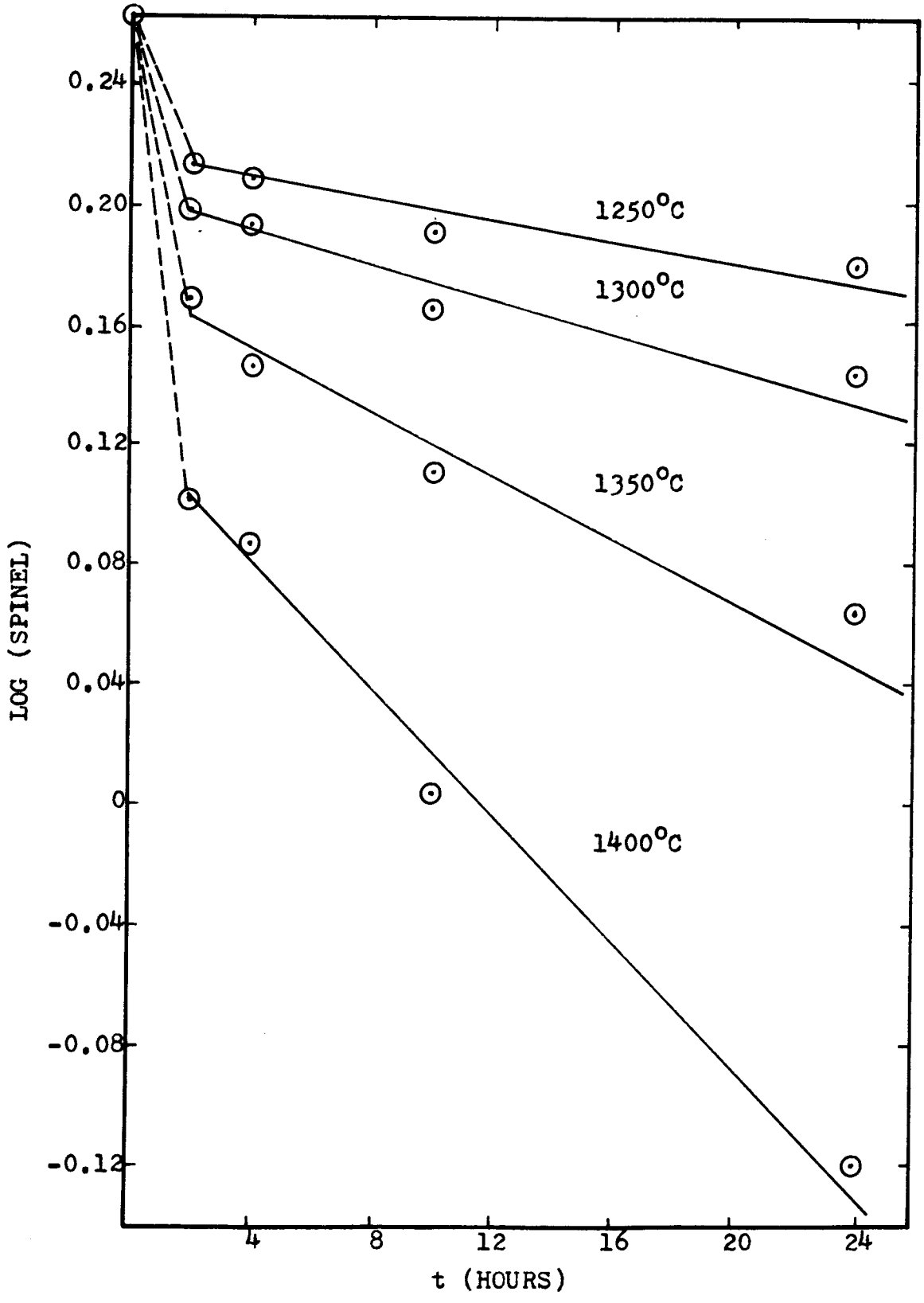

Figure 14. First Order Reaction of Composition (5).

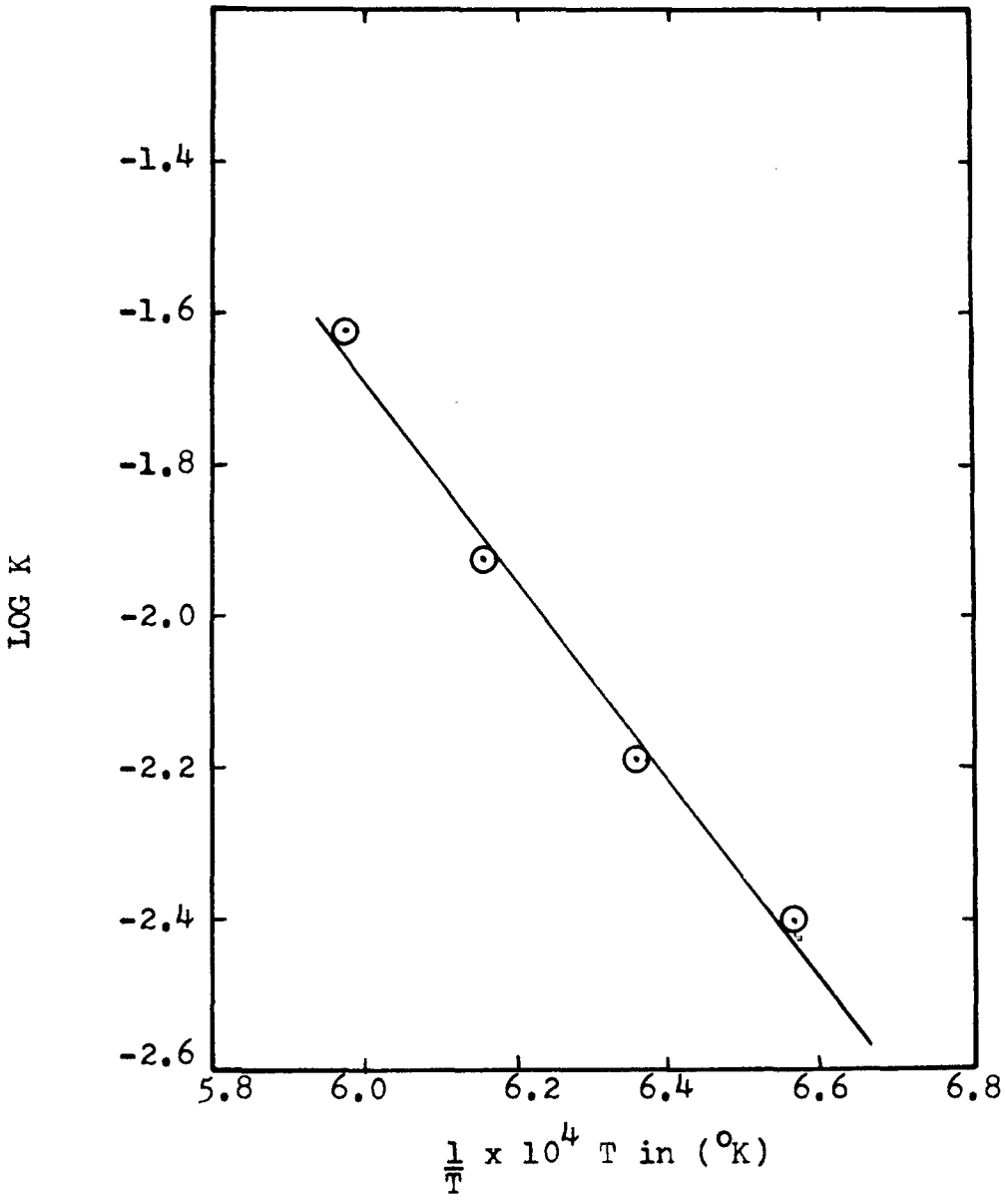

Figure 15. Reaction of Composition (5) From Which The Arrhenius Activation Energy May Be Calculated.

To compare the effect of zircon addition, composition 4 may be compared to composition 1 in addition to comparing composition 5 to composition 2 since the only difference in the two sets of reactions was the zircon content. Room temperature x-ray diffraction patterns showed that the concentration of zircon appeared to remain constant throughout the heating schedule up to 1350°C. At this temperature the concentration of zircon decreased presumably as a result of glass formation. The cordierite content for the compositions 4 and 5, which contain zircon, increased slightly above the composition 1 and 2, not containing zircon, between 1350° and 1400°C as a consequence of zircon addition, Figs. 16 and 17. An explanation of this phenomena may have been that glass formed a liquid phase which promoted diffusion and hence increased the cordierite content of the body.

Reactions of Forsterite, Mullite and Silica

To compare cordierite formation using starting phases other than spinel and silica, a composition was formulated from forsterite, mullite and fused silica as follows:

$$\underset{\text{(Forsterite)}}{3(2MgO.SiO_2)} + \underset{\text{(Mullite)}}{2(3Al_2O_3.2SiO_2)} + \underset{\text{(Silica)}}{8SiO_2} \longrightarrow \underset{\text{(Cordierite)}}{3(2MgO.2Al_2O_3.5SiO_2)} \quad (19)$$

Quantitative cordierite analysis was performed after 24 hours at various temperatures, Table 10. Also shown in Table 10 are qualitative analysis of all x-ray detectable phases. From the phases present it is apparent that many parallel reactions were proceeding and probably the major reaction forming cordierite was not reaction (19) at all.

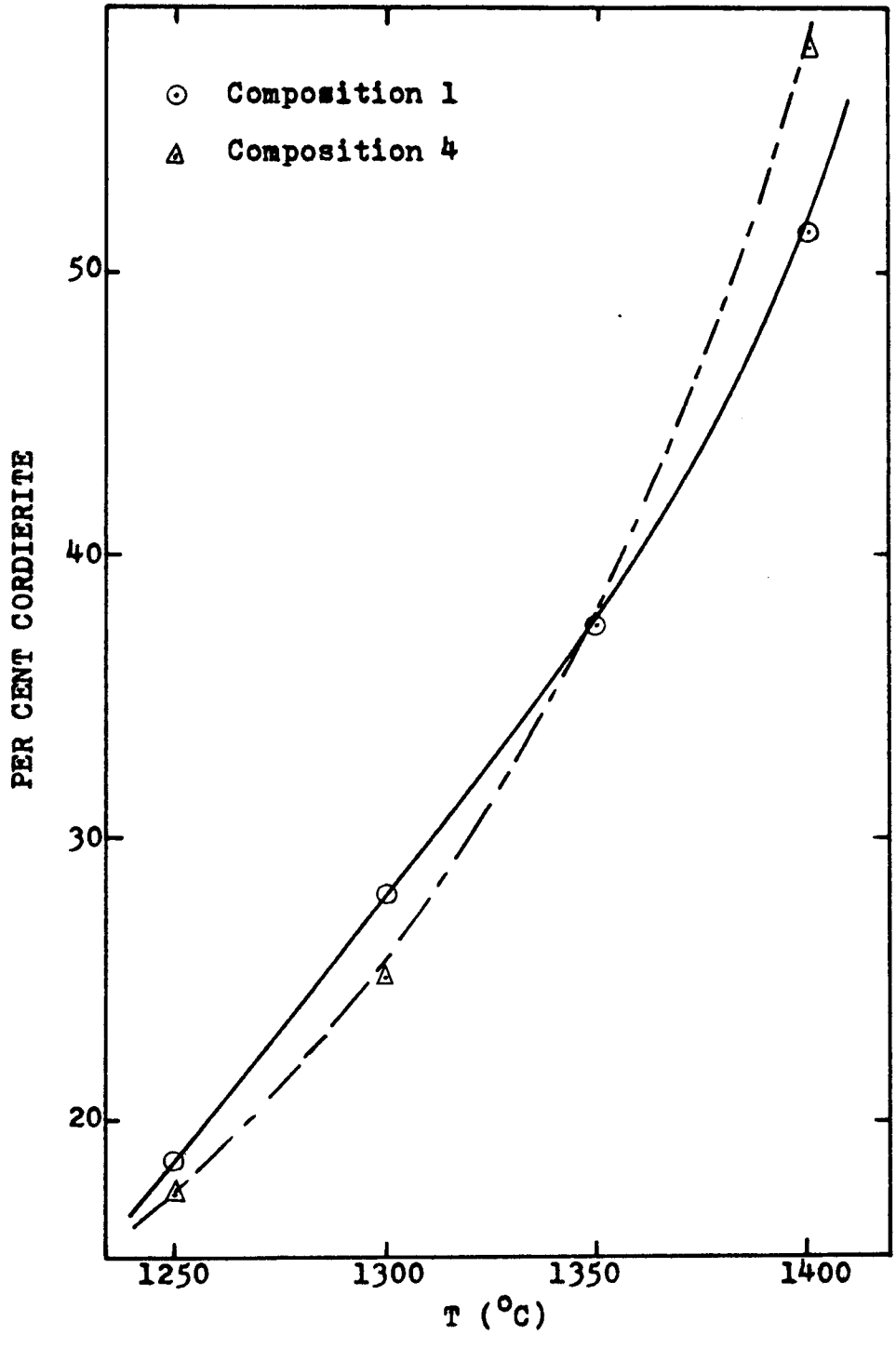

Figure 16. Cordierite Content for Compositions (1) and (4) After 24 Hours

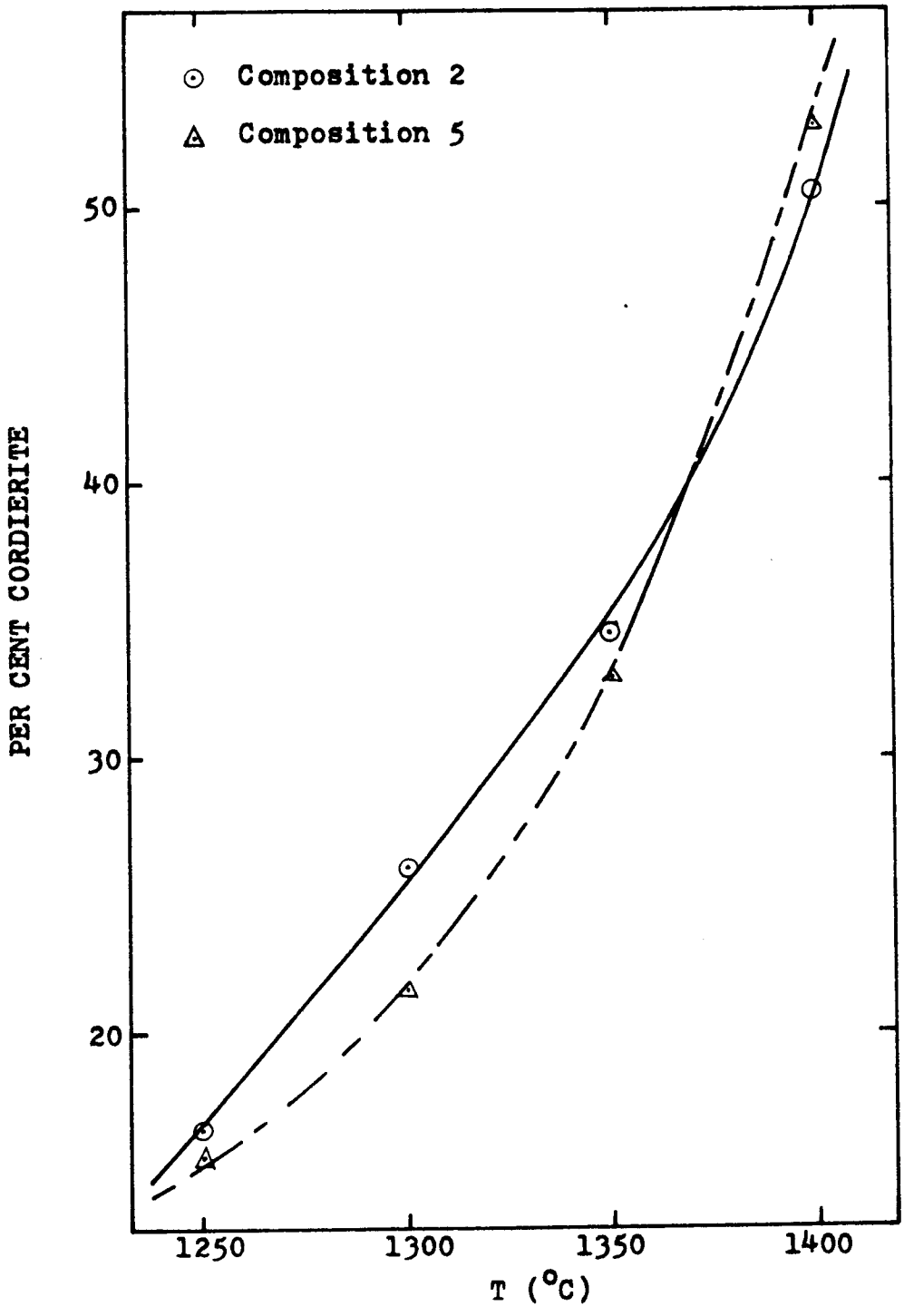

Figure 17. Cordierite Content for Compositions (2) and (5) After 24 Hours.

Table 10. Phase Analysis for Compositions 3 and 6

Temperature (°C)	Phases Present					
	MgO	Forsterite	Enstatite	Cordierite (Weight %)	Cristobalite	Mullite
1250	Small	Medium	Medium	23.0	Large	Medium
1300	Smaller	Small	Medium	37.5	Medium-large	Small
1350	Trace	Trace	None	63.3	Medium	Trace
1400	Trace	None	None	77.5	Trace	None

Other possible reactions were the following:

$$2MgO.SiO_2 \longrightarrow MgO.SiO_2 + MgO \quad (20)$$

(Forsterite) (Enstatite)

$$2MgO.SiO_2 + SiO_2 \longrightarrow 2(MgO.SiO_2) \quad (21)$$

$$MgO + SiO_2 \longrightarrow MgO.SiO_2 \quad (22)$$

$$SiO_{2(g)} \longrightarrow SiO_{2(c)} \quad (23)$$

$$6(MgO.SiO_2) + 2(3Al_2O_3.2SiO_2) + 5SiO_2 \longrightarrow 3(2MgO.2Al_2O_3.5SiO_2) \quad (24)$$

$$6MgO + 2(3Al_2O_3.2SiO_2) + 11SiO_2 \longrightarrow 3(2MgO.2Al_2O_3.5SiO_2) \quad (25)$$

Room temperature x-ray diffraction patterns indicated the following:

1. MgO was formed by equation (20). The evidence for this explanation are: a) MgO was not used as a raw material, b) most MgO was formed at 1250°C, c) the presence of enstatite.
2. Enstatite formed by equation (22) was minimal because MgO and SiO_2 are present at 1350° and 1400°C, but no enstatite was detected at these temperatures.
3. Some crystalline cordierite may have formed by reaction (25) because of decrease in MgO, SiO_2 and mullite from 1350° to 1400°C. Equation (25) was not important because MgO content was always small.
4. Equation (24) was probably the dominant reaction for cordierite formation

because enstatite content was constant between 1250^{o} and 1300^{o}C and not detectable at 1350^{o}C. Obviously enstatite was readily going to cordierite by reaction (24) between 1300^{o} and 1350^{o}C. In order for enstatite to remain constant between 1250^{o} and 1300^{o}C, forsterite must have been converting to enstatite rather than forming cordierite by reaction (19).

In all cases mullite was forming cordierite because no other Al_2O_3 containing phases were detected and mullite decreased as cordierite increased. As in all other cases SiO_2 glass converted to cristobalite and crystalline cordierite was formed consuming cristobalite.

Cordierite formation was faster using forsterite, mullite and fused silica as starting materials than from spinel and fused silica for raw materials of approximately the same particle size, Fig. 18. Addition of zircon for the mullite, forsterite and silica reaction showed higher reaction rates but, because of the quantity of mullite and forsterite available to form cordierite has been diluted, the amount of crystalline cordierite developed was slightly less. Figure 18 also indicated that in composition 3 and 6, cordierite content has increased to the point (1350 - 1400^{o}C) that cordierite formation was limited by a lack of reactant materials.

The results obtained in this investigation indicated that the availability of mullite is not a key factor in the formation of cordierite, but it depends largely on which intermediate phases develops from the raw materials used for cordierite formation. In our case no mullite was detected at any temperature in the formation of cordierite from spinel and cristobalite. This is significant because of Sorrel's implication that cordierite development is primarily dependent on the availability

of mullite (12). The reaction of mullite, enstatite and cristobalite leading cordierite showed faster rate and increased the amount of crystalline cordierite developed.

Smaller cordierite content was obtained than for industrial compositions (14). This is because particle size for clay and talc is lower than that of the raw materials used in this work.

CHAPTER V

CONCLUSIONS AND RECOMMENDATIONS

Conclusions

From reactions using spinel and fused silica, as starting raw materials to form cordierite, the following was concluded:

1. Reaction rate of spinel with silica glass was faster than with cristobalite.
2. Spinel and cristobalite reacted to form cordierite.
3. The rate law for the spinel and cristobalite reaction followed a first order reaction with respect to spinel.
4. Any excess silica in a ceramic body approaching the theoretical composition of cordierite reduced the amount of crystalline cordierite developed.
5. No mullite was detected at any temperature on heating spinel and cristobalite to form cordierite.

Where mullite, forsterite and fused silica were the starting raw materials, it was concluded:

6. The primary reaction forming cordierite was between enstatite, mullite and cristobalite.
7. No spinel was detected at any temperature from the forsterite, mullite and cristobalite reaction leading to cordierite.

Conclusions based on all reactions investigated were:

8. Cordierite formed faster with mullite, forsterite and fused silica than from

spinel and fused silica for initial materials of approximately the same particle size.

9. Addition of 5% of zircon indicated an increase of the amount of cordierite developed between 1350^{o} and 1400^{o}C, but at 1350^{o}C and below, zircon was a detriment to cordierite formation for all reactions.
10. Cordierite development is primarily dependent on temperature, the availability of intermediate phases responsible for cordierite formation and time of firing.

Recommendations

Additional studies of the rate law for the enstatite, mullite and cristobalite reaction are required for a better understanding for cordierite formation when such intermediate phases are responsible in developing crystalline cordierite. Ground raw materials have to be extremely small in particle size (-325 mesh), in order to carry out intimately mixing of fine particles and well mixed to achieve homogeneity. The composition of the raw materials should be in the proportion corresponding to the theoretical formula of cordierite. Any excess of silica reduces the amount of cordierite developed.

Investigations of prolonged heating at the temperature at which intermediate phases react to form cordierite are necessary to study optimum conditions for cordierite formation.

APPENDIX A

RAW MATERIALS

The particle size of the raw materials are given in Table 11. Compositions of the bodies made were approximately of the same particle size, so the effect of particle size comparing the results obtained for each composition were neglected.

Table 11. Raw Materials

Raw Material	Particle Size (Mesh)
Spinel (i)	-325
Forsterite (i)	-100
Mullite (i)	-100
Fused Silica GP-3 I (i)	35% less than 2 microns
Zircon (ii)	29% less than 1 micron

(i) Glassrock Products Incorporated, Atlanta.

(ii) Ultrox Std. M & T Chemicals Inc., Atlanta.

APPENDIX B

PREPARATION OF CORDIERITE STANDARD

A standard sample of 100% crystalline cordierite was prepared by Ferro Corporation, Technical Center, using the raw materials given in Table 12. The batch yielded theoretical cordierite on heating. The batch was dry ball milled in a porcelain jar for two hours, melted at 1600°C for two hours in a platinum crucible and water quenched. The glass was crushed to -100 mesh, remelted at 1600°C for two hours and then recrushed to pass a 100 mesh screen. The glass was devitrified at 1300°C for 20 hours to give 100% cordierite (23).

Table 12. Composition Used in Preparing Cordierite Standard

Material	Supplier
Calcined Alumina	Alcoa A-14
Powdered Quartz	Pennsylvanian Glass Sand Co.
Magnesium Carbonate	Michigan Chemical Co.

Table 13. Experimental Conditions for Room Temperature X-ray Diffraction Analysis

Factor	Setting
Killivolts	35 Kv
Milliamperes	15 ma
Time constant	4
Scale Factor	1×10^3
Chart Speed	1/2 inch/minute
Scan Speed	$1/4^o$ 2θ/minute (Quantitative Analysis)
	1^o 2θ/minute (Qualitative Analysis)
Radiation	Copper K_α
Filter	Nickel

Table 14. Experimental Conditions for High Temperature X-ray Diffraction Analysis (21).

Factor	Setting
Killivolts	50 Kv
Milliamperes	20 ma
Time constant	2.0
Scan Speed	2^{o} 2θ/minute
Radiation	Copper K_{α}
Heating Rate	500^{o}F/Hour

APPENDIX D

QUANTITATIVE X-RAY DIFFRACTION DATA

The following data were collected from quantitative x-ray diffraction of the samples. The values given previously are the average of two determination in each run indicated by the ratio of the peak intensity and the number of counts of the peak size of cordierite to that of strontium fluoride. The major cause of differences were due to experimental techniques as preparation of the samples to be mounted for x-ray diffraction. The experimental condition for the x-ray quantitative analysis of crystalline cordierite are given in Appendix C.

The percentage reproducibility between differences of the data obtained from the ratios of the peak height and peak area was $\pm$ 1.15%.

Table 15. Cordierite Content at 1250°C (Weight Percent)

Composition	Cordierite Peak Area / SrF_2 Peak Area	Cordierite Peak Height / SrF_2 Peak Height
1-2	12.0	11.0
1-4	12.0	12.0
1-10	15.0	15.0
1-24	19.0	18.0
2-2	10.0	9.0
2-4	12.0	11.0
2-10	13.0	12.0
2-24	18.0	15.0
3-24	25.0	23.0
4-24	18.0	17.0
5-2	10.0	9.0
5-4	10.0	11.0
5-10	14.0	13.0
5-24	16.0	15.0
6-24	22.0	22.0

Table 16. Cordierite Content at 1300°C (Weight Percent)

Composition	Cordierite Peak Area / SrF_2 Peak Area	Cordierite Peak Height / SrF_2 Peak Height
1-2	15.0	15.0
1-4	15.0	15.0
1-10	22.0	20.0
1-24	30.0	26.0
2-2	13.0	13.0
2-4	16.0	15.0
2-10	18.0	18.0
2-24	27.0	25.0
3-24	38.0	37.0
4-24	26.0	24.0
5-2	13.0	12.0
5-4	13.0	13.0
5-10	19.0	17.0
5-24	22.0	21.0
6-24	36.0	39.0

Table 17. Cordierite Content at 1350°C (Weight Percent)

Composition	$\frac{\text{Cordierite Peak Area}}{SrF_2 \text{ Peak Area}}$	$\frac{\text{Cordierite Peak Height}}{SrF_2 \text{ Peak Height}}$
1-2	20.0	20.0
1-4	23.0	23.0
1-10	28.0	26.0
1-24	38.0	37.0
2-2	17.0	17.0
2-4	19.0	19.0
2-10	28.0	25.0
2-24	36.0	33.0
3-24	65.0	64.0
4-24	40.0	36.0
5-2	18.0	18.0
5-4	21.0	21.0
5-10	28.0	25.0
5-24	33.0	33.0
6-24	64.0	60.0

Table 18. Cordierite Content at 1400°C (Weight Percent)

Composition	$\frac{\text{Cordierite Peak Area}}{SrF_2 \text{ Peak Area}}$	$\frac{\text{Cordierite Peak Height}}{SrF_2 \text{ Peak Height}}$
1-2	29.0	26.0
1-4	34.0	32.0
1-10	44.0	38.0
1-24	54.0	49.0
2-2	24.0	24.0
2-4	33.0	29.0
2-10	39.0	37.0
2-24	52.0	49.0
3-24	80.0	73.0
4-24	59.0	57.0
5-2	29.0	27.0
5-4	31.0	29.0
5-10	42.0	39.0
5-24	52.0	54.0
6-24	82.0	75.0

BIBLIOGRAPHY

1. Lamar, R. S., "Development of Cordierite Bodies with Sierralite, a New Ceramic Material," J. Am. Ceram. Soc., 32, 65 (1949).

2. Krönert, W. Schwiete,H.E., and Suckow, A., "Die Bildung von Cordierit aus Talk, Kaolin und den Oxiden im Dreistoffsystem $MgO-Al_2O_3-SiO_2$," Ber. DKG, 38, 420-425 (1964).

3. Byström, A., "The Crystal Structure of Cordierite," Arkiv For Kemi, Mineralogi Och Geologi Band 15B., 12.

4. Gibbs, G. V., "The Polymorphism of Cordierite. The Crystal Structure of Cordierite," Am. Mineral., 51, 1068 (1966).

5. Karkhanavala, M. D. and Hummel, F. A., "The Polymorphism of Cordierite," J. Am. Ceram. Soc., 36, 389-392 (1953).

6. Yoder, H S., "The $MgO-Al_2O_3-SiO_2-H_2O$ System and Related Metamorphic Facies," Am. J. Sci., 250, 569-627 (1952).

7. Miyashiro, A., "Cordierite-Indialite Relations," Am. J. Sci., 255, 43-62 (1957).

8. Espinoza and Aza, "Materiales Ceramicos de Cordierita," Soc. Esp. de Cer., 731 (1967).

9. Lamar, R. S. and Warner, M. F., "Reaction and Fired-Property Studies of Cordierite Compositions," J. Am. Ceram. Soc., 37, 602 (1954).

10. Foster, W. R., "Contribution to the Interpretation of Phase Diagrams by Ceramist," J. Am. Ceram. Soc., 34, 151 (1951).

11. Hubertus, H. and Lidkoping, "Methods of Developing a dense Cordierite Body," Sprechsaal, 97, 145 (1964).

12. Sorrel, A., "Reaction Sequence and Structural Changes in Cordierite Refractories," J. Am. Ceram. Soc., 43, 337 (1960).

13. Green, A. T. and Stewart, G. H., "Ceramics a Symposium," Brit. Ceram. Soc., 694 (1953).

14. Beals, R. J. and Cook, R. L., "Low-Expansion Cordierite Porcelains," J. Am. Ceram. Soc., 35, 53 (1952).

15. Davis, M. P. and Hackler, W. C., "Correlation Between Physical Properties and Thermochemical Reactions in a Mullite-Cordierite Composition," Am. Ceram. Soc. Bull., 40, 362 (1961).

16. Kingery, W. D., Introduction to Ceramics, 473 (1960).

17. Ford, F. W., The Effect of Heat on Ceramics, Institute of Ceramics Textbook Series, 69 (1967).

18. Thurnauer, H., "Properties and Uses of Technical Ceramics," Materials and Methods, 87 (1947).

19. Daniels, F. and Alberty, R. A., Physical Chemistry, 325 (1967)

20. Taylor, W. N.,"Reactions Between Solids in The Absence of a Liquid Phase," J. Am. Ceram. Soc., 17, 155 (1934).

21. Parmelle, J. D., Harbison-Walker Refractories, Garber Research Center, Pittsburgh, Pa., Personal Communication, July 10, 1972.

22. Brown, S. D., and Kistler, S. S., "Devitrification of High-SiO_2 Glasses of the System Al_2O_3-SiO_2," J. Am. Ceram. Soc., 42, 263 (1959).

23. Beal, D. F., Ferro Corporation, Technical Center, Independence, Ohio, Personal Communication, June 19, 1972.